Radiocarbon dating of soil archives

van der Plicht, J.; Streurman, H. J.; van Mourik, J. M.

Published in:
Reading the Soil Archives

DOI:
10.1016/B978-0-444-64108-3.00003-3

Publication date:
2019

CHAPTER

3

Radiocarbon dating of soil archives

J. van der Plicht[a,*], *H.J. Streurman*[a], *J.M. van Mourik*[b]

[a]Centre for Isotope Research, University of Groningen, Groningen, the Netherlands; [b]Institute for Biodiversity and Ecosystem Dynamics (IBED), Faculty of Science, University of Amsterdam, Amsterdam, the Netherlands

*Corresponding author.

3.1 The theory of radiocarbon dating of soil organic matter

3.1.1 Introduction

This chapter reviews the radiocarbon method with an emphasis on dating soil organic matter and its intrinsic difficulties. Both ^{14}C measurement techniques (conventional and accelerator mass spectrometry (AMS)) are presented and discussed. This includes the present state of the art of the radiocarbon dating method on timescale calibration, sample quality aspects and sample pretreatment. In addition, the stable isotope ^{13}C can be used as a tracer for geochemical processes. Applying both carbon isotopes in soil science is illustrated by selected case studies.

The radiocarbon (^{14}C) dating method was developed around 1950 (Libby, 1952; Taylor et al., 1992). The method enables direct dating of organic remains back to about 50,000 years ago. Since that time, several 'revolutions' have improved the method considerably. Amongst the most significant are the introduction of AMS in the 1980s, and calibration of the ^{14}C timescale to obtain absolute dates.

AMS enables small (milligram size) sample analysis (Tuniz et al., 1998; Jull, 2013). This is a factor of 1000 less than the original so-called conventional method based on radiometry (Cook and van der Plicht, 2013). AMS therefore enables ^{14}C dating of precious fossils, such as archaic human bones and artefacts, as well as intrinsically small samples, such as botanical remains (macrofossils and seeds) and fragments (e.g., Wagner et al., 2018).

Calibration now enables absolute dating back to 50,000 years ago (Reimer et al., 2013), i.e., the complete dating range. In turn, this has spawned 'revolutions' in applications, amongst which are archaeology, palaeontology and Quaternary geology. Radiocarbon provides a 'yardstick of time', enabling the measurement of past time by scientific means, independent of associations and assumptions. This enables synchronization and chronological comparison of different areas at excavation sites and also between sites and regions. This is essential for proper interpretation of archaeological or stratigraphical layers and association with data from other fields (e.g., van der Plicht and Bruins, 2001).

Reading the Soil Archives
https://doi.org/10.1016/B978-0-444-64108-3.00003-3

While the method is basically simple, it is complex in detail and errors in matters concerning both fieldwork and technical laboratory aspects. Therefore stringent quality control is necessary to build up reliable ^{14}C chronologies. This involves regular laboratory intercomparisons, duplicate measurements of samples, issues such as conventional dating versus AMS, sample selection, association and others (van Strydonck et al., 1999; Scott et al., 2010). In addition to ^{14}C dating, the content of the stable carbon isotope ^{13}C of the sample is also measured. For some applications this is complemented by the stable isotope ^{15}N (Fry, 2008). Both stable isotopes provide insight into topics such as palaeoecological conditions and geochemical processes. Also, the stable isotope ^{18}O is a geochemical tracer, in particular for carbonates and aquatic reservoirs (Mook, 2006).

In this section, a short review of the principles of the ^{14}C method and conventions is given. The application discussed here is dating of soil organic matter. This category of samples shows intrinsic problems. The use of the stable isotope ^{13}C in soil science is illustrated as well. Selected case studies will be discussed.

3.1.2 The ^{14}C dating method

The element carbon consists of three naturally occurring isotopes: ^{12}C, ^{13}C and ^{14}C with abundances of ca. 98.9%, 1.1% and 10^{-10}%, respectively. The isotope ^{14}C (radiocarbon) is continuously produced in the earth's atmosphere by cosmic radiation. Radiocarbon is radioactive and decays with a half-life of 5730 ± 40 years (Godwin, 1962). A stationary state of production, distribution between the main carbon reservoirs (atmosphere, ocean and biosphere) and decay result in a more or less constant ^{14}C concentration in atmospheric CO_2 and the terrestrial biosphere (e.g., Mook and Waterbolk, 1985; Mook and van de Plassche, 1986). Upon the death of an organism, the radioactive ^{14}C decays, and by measuring the amount of remaining ^{14}C in the sample its time of death can be derived. For accurate radiocarbon dating, only the ^{14}C that was part of the organism when it died should be measured. This requires so-called pretreatment of the sample.

It has been known for some time that the ^{14}C concentration of atmospheric CO_2 has not always been the same. In tree rings, natural variations of atmospheric $^{14}CO_2$ abundance were discovered on a timescale of one decade to a few centuries (de Vries, 1958). Later, it was discovered that these variations can be attributed to variations in solar activity (Stuiver, 1965), which in turn influence the production of ^{14}C in the atmosphere. Also, changes in the geomagnetic field strength influence the production of ^{14}C in the atmosphere (Bucha, 1970). This is understood because both solar activity and geomagnetic field strength determine the amount of cosmic radiation impinging on the earth (van der Plicht, 2013). In addition, atmospheric $^{14}CO_2$ concentration also depends on exchange between the atmosphere and ocean.

Because of these variations in the natural ^{14}C concentration, the ^{14}C clock runs at a varying pace, different from real clocks: ^{14}C time is not equivalent to calendar time. Therefore the ^{14}C timescale has been defined and needs to be calibrated to establish the relationship between ^{14}C time and historical time.

This definition is known as the 'radiocarbon convention' (Mook and Streurman, 1983; van der Plicht and Hogg, 2006; Mook and van der Plicht, 1999). The definition states that ^{14}C radioactivity is always measured relative to that of a standard (oxalic acid with a radioactivity of 0.226 Bq/gC), representing modern natural radiocarbon, which corresponds to AD 1950. From this measured radioactivity the 'radiocarbon age' is calculated using a half-life of 5568 years. This value was used in the early days of ^{14}C dating and is not correct; the proper value was later established as the aforementioned 5730 years. However, it is still used to

avoid confusion; the error in the 'date' that is introduced this way is corrected by calibration (see later).

Other complications arise from the differences in processes in nature and the laboratory for the different isotopes, caused by their different masses. This is known as 'fractionation'. For example, in biological pathways, lighter isotopes are taken up preferentially, reducing the proportion of ^{14}C in a sample making it seem older. The proportion of ^{13}C is also changed. This isotope is stable, i.e., its concentration is constant throughout time. Therefore the ratio of the stable isotopes ^{13}C and ^{12}C in a sample can be used to estimate the fractionation effect of ^{14}C. The radiocarbon convention implies that the fractionation correction must be to a standardized value for the $^{13}C/^{12}C$ ratio (to $\delta^{13}C = -25‰$; the δ values are introduced later, and see Mook, 2006).

In the following we will use the 'activity ratio' ^{14}a. This is defined as the ^{14}C radioactivity of the sample relative to that of the standard, and taking into account the convention. Thus for the oxalic acid standard, $^{14}a = 1$ or 100%; for a sample with a (conventional) half-life of 5568 years, $^{14}a = 0.5$ or 50% (Mook and van der Plicht, 1999).

The defined conventional ^{14}C timescale is expressed in the unit BP. This originally meant 'Before Present'. The expression 'Present', originally taken as AD 1950, should not be taken literally, because the relation between the ^{14}C timescale and the calendar timescale is complex. This relation is determined by calibration.

3.1.3 Timescale calibration

Calibration involves measuring samples by both the ^{14}C method (reported in BP by the convention) and another method. Ideally, this other method has to be independent from ^{14}C, yielding absolute dates (in AD/BC), and the samples have to be from the terrestrial (or atmospheric) reservoir. The paired dates (BP and AD/BC) then are used to construct a calibration curve, which gives the relationship between both timescales. For the dates calibrated using this curve, the chosen convention values for half-life and fractionation correction are taken into account.

The unit calBP is used as well; this is defined as calendar years relative to AD 1950 (calBP = AD − 1950).

The ideal samples for calibration are tree rings, because they can be dated absolutely by means of dendrochronology. Following the early work of Suess (1980), the ^{14}C community distributed special issues of the journal *Radiocarbon* with calibration curves based on a variety of available records. These issues are updated regularly. The main data are tree rings dated by both ^{14}C and dendrochronology. Beyond the available absolutely dated dendrochronological dataset, records from varves (laminated sediments containing botanical remains), plus corals/foraminifera and speleothems, which are also dated by isotopes in the uranium decay chain, are used. The main varved record is from the terrestrial sediment of Lake Suigetsu in Japan (Bronk Ramsey et al., 2012).

Using these datasets, the calibration curve named IntCal13 has been constructed. It is the presently recommended calibration curve, and is shown in Fig. 3.1.1. It will be replaced shortly by IntCal20 (Reimer et al., 2020). Significant changes will be implemented for the oldest part of the curve. The dendrochronological part and the part derived from other records are indicated, separated at 13,900 calBP (Reimer et al., 2013).

The long-term (millennia scale) trend of the calibration curve is explained by the changing geomagnetic field. On this long-term trend, modulations on the century/decennium scale (known as 'wiggles') can be seen, which are caused by fluctuations in solar activity. There was significantly more ^{14}C present in nature millennia ago, causing ^{14}C ages to be 'young': 46,000 ^{14}C years ago (in BP) corresponds to

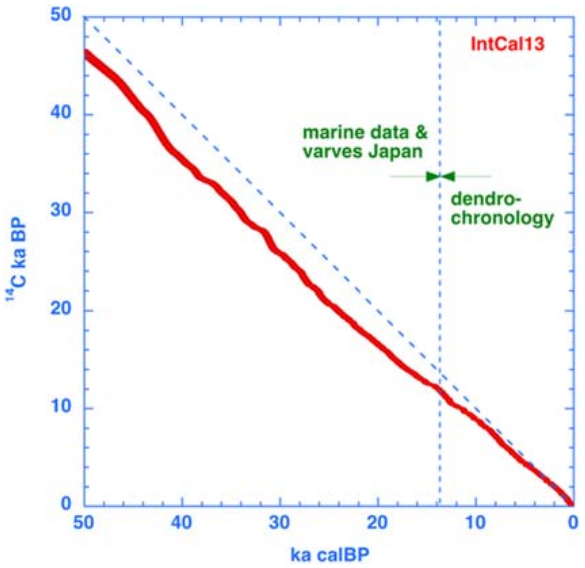

FIGURE 3.1.1 The calibration curve IntCal13, to be used for transferring ^{14}C dates (vertical, BP) into calendar ages (horizontal, calBP = AD − 1950).

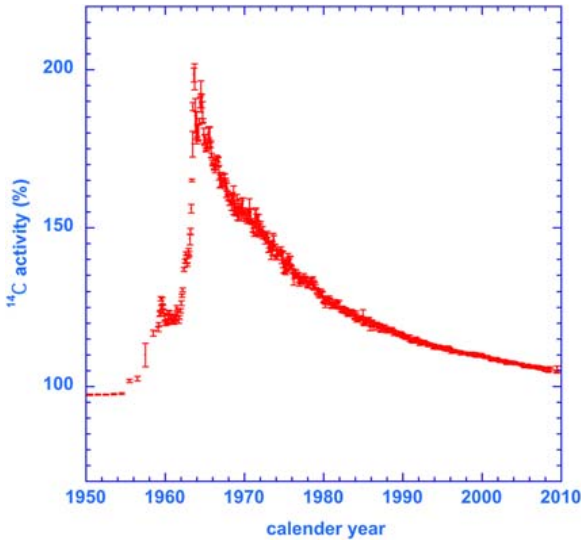

FIGURE 3.1.2 Measurements of atmospheric ^{14}C content for modern times, showing the 'bomb peak'.

about 50,000 calendar years ago (in calBP). This is obviously important for the interpretation of Pleistocene samples.

In modern times, the ^{14}C content in nature is influenced by anthropogenic effects. First, in the atmosphere and terrestrial samples, the greenhouse gas emissions (which are of geological age and thus do not contain ^{14}C) have diluted the natural atmospheric $^{14}CO_2$ content since around AD 1900. This is known as the Suess effect, which is also apparent in terrestrial samples like tree rings (Stuiver and Quay, 1981). Furthermore, after the Second World War, test explosions of nuclear bombs in the atmosphere produced extra ^{14}C. In the Northern Hemisphere this increased the ^{14}C concentration by a factor of two in 1963 (Fig. 3.2.2).

Since 1963 atmospheric explosions no longer occurred (except for a few small bomb tests), so the ^{14}C content decreased in the atmosphere and increased in the oceans by exchange of $^{14}CO_2$ (e.g., Levin and Hesshaimer, 2000). The atmospheric ^{14}C signal for the years 1950–2010 is shown in Fig. 3.1.2. It shows what is generally known as the 'bomb peak' and is valid for the Northern Hemisphere (Hua et al., 2013). At present, the interplay of ^{14}C in the global carbon cycle (bomb peak, fossil fuels and the reservoirs' atmosphere, biosphere and the oceans) causes natural ^{14}C content in the atmosphere close to 'normal', defined as $^{14}a = 100\%$ (Graven, 2015).

Examples of 'bomb dating' of soil organic carbon can be found in Trumbore et al. (1989). The ^{14}C isotope can be used as a tracer for carbon (geo)chemistry.

3.1.4 Measuring carbon isotopes

For accurate ^{14}C dating, only the ^{14}C that was part of the organism when it died should be measured. Therefore the first task is to remove any foreign carbon that entered the sample since that time. Such contamination comes principally from the burial environment. This is done by a mixture of physical and chemical means using pretreatment protocols. These procedures also isolate a stable chemical fraction of a sample – for example, collagen from bone, or cellulose

from wood. The treatment of soil organic matter is discussed later. For a complete description of sample pretreatment aspects we refer to Mook and Streurman (1983) and Mook and van de Plassche (1986).

The next stage in dating is combustion of the isolated and purified datable fraction of the sample to produce CO_2. This CO_2 gas contains the ^{14}C from the sample; dating is the measurement of this amount of ^{14}C.

For the conventional method, the ^{14}C radioactivity in the CO_2 is measured by radiometry. This ^{14}C radioactivity is extremely low. Therefore special counters in a low-background setup are required, designed to shield the natural radioactivity. This method typically requires a litre of CO_2 gas, roughly equivalent to a gram of carbon, or grams of sample material. The conventional radiometric method was developed around 1950. For more technical details of the conventional method we refer to Mook and Streurman (1983) and Cook and van der Plicht (2013).

AMS is a form of mass spectrometry which measures the ^{14}C content directly instead of those ^{14}C atoms which decay by radioactivity. Mass spectrometry is much more efficient than radiometry, which enables a very significant reduction (by a factor of 1000) in sample size to typically 1 mg of carbon. The AMS technique was developed in the 1980s (Tuniz et al., 1998; Bayliss et al., 2004; Jull, 2013).

For AMS, the principles of chemical/physical pretreatment are the same as for the conventional method. However, for AMS, one extra step is needed: the CO_2 gas needs to be reduced to graphite (Aerts et al., 2001). The graphite is pressed into targets, mounted in a sample wheel before it is loaded into the ion source of the machine.

Using a high voltage, the AMS accelerates the C ions to high energies. A set of magnets separates this high energy beam of C ions according to mass: 12, 13 and 14 for the isotopes ^{12}C, ^{13}C and ^{14}C, respectively. The ^{12}C and ^{13}C beams are measured by current meters, and from this the ratio $^{13}C/^{12}C$ is determined. This is used for fractionation correction, necessary for ^{14}C dates. A particle detector measures the ^{14}C counts, so that the $^{14}C/^{12}C$ ratio can also be determined. Further technical details, performance and status reports of the Groningen AMS facility can be found in van der Plicht et al. (2000) and references therein. From all of this, the ^{14}C ages in BP are calculated (Mook and van der Plicht, 1999). Note that both ^{14}C measuring methods (radiometry and mass spectrometry) yield numbers in BP, which have the same meaning.

For conventional dates, the CIO laboratory code GrN is used; for AMS dates, this is GrA.

Stable isotope concentrations are measured by conventional mass spectrometry based on molecular gases. The stable carbon isotope (^{13}C) content of the sample is measured in CO_2 by isotope ratio mass spectrometry upon combustion of the pretreated ^{14}C sample material (such as collagen, prepared from fossil bone). Thus the same CO_2 is used for both isotope measurements, ^{13}C and ^{14}C dating – either by AMS or by the conventional method.

The stable isotopic content of the samples is expressed in delta (δ) values, which are defined as the deviation (expressed in per mil) of the rare to abundant isotope ratio from that of a reference material:

$$\delta^{13}C = (^{13}C/^{12}C)_{sample}/(^{13}C/^{12}C)_{reference} - 1(\times 1000‰)$$

The absolute isotope content of the reference materials has been measured very accurately (Mook, 2006 and references therein). For ^{13}C, the reference material is Pee Dee Belemnite carbonate, the carbonate from a belemnite found in the Cretaceous Pee Dee formation of North America (Mook, 2006; Fry, 2008).

Apart from fractionation correction for ^{14}C dating, the stable isotope ratio $\delta^{13}C$ has merit by itself. As will be shown in selected case

studies, this isotope can be used as a tracer for geochemical processes (Michener and Lajtha, 2007; Fry, 2008).

3.1.5 Chemical aspects of samples

Not all types of material are equally suitable for radiocarbon dating. For example, from a geophysical point of view, a sample has a certain degree of association with the event to be dated (Mook and Streurman, 1983; Olsson, 1989; van Strydonck et al., 1999). From a physical point of view, ^{14}C ages may have different degrees of reliability because, for example, the original ^{14}C age of the sample is not well known (which is the case for groundwater). From a chemical point of view, the sample may contain foreign carbon having a different ^{14}C content (for example, humic substances of plant roots from stratigraphically lower depths).

In general, the contaminant has a higher (often 'modern') ^{14}C concentration, which will result in a date which is too young. On the other hand, admixture of zero-activity bituminous products or graphite ('dead') in the sample will result in a date which is too old. Both are known to happen.

One can calculate how much contamination is needed to explain aberrant dates. It obviously depends on the age of the contaminant, which theoretically can be any age between modern and fossil. Let us assume here modern contamination, then a contamination of 1% modern carbon in a sample of 50,000 BP will be measured as 35,000 BP. Further examples can be found in Mook and Streurman (1983) and Mook and van de Plassche (1986). These articles were written for the conventional dating method, using large samples. For our example, 1% foreign carbon for a 1 g sample is 10 mg, which is relatively large. The same calculations apply to AMS but the samples are much smaller. Here, a contamination of 1% foreign carbon for a 1 mg sample is only 10 μg; AMS is obviously much more sensitive for contamination (Lanting and van der Plicht, 1994).

Samples to be dated need pretreatment to remove contaminants. The form and intensity of pretreatment depend on the type, quality and quantity of the sample. An example of physical pretreatment is the removal of subrecent plant roots. Chemical pretreatment is designed to isolate the pure datable fraction of the sample. The standard chemical recipe is the so-called acid-alkali-acid (AAA) method, also known as acid-base-acid. This is applied to most sample materials. The sample material is subjected to the following extraction steps:

1. A 4% HCl solution to remove soil carbonate and infiltrated humic (fulvic) acids;
2. A 4% NaOH solution to remove components like tannic acids and lignin;
3. A 4% HCl to remove any CO_2 absorbed during step 2.

Standard usually means also a temperature of 80°C for 24 h for each step; however, this is often too rigorous, so that too much sample material will dissolve. A lower temperature, duration and/or a more diluted acid/base can be applied in such cases. Pretreatment by step 1 only is referred to as A treatment.

3.1.6 Soil organic carbon

In mineral humous soil horizons, no plant remains are recognizable. The mineral matrix may be sand, clay or löss. The organic content consists mainly of fulvic and humic acids and humin (see later).

Plants and wood have an organic carbon content of about 50% (Mook and Streurman, 1983). Compared with such sample materials, that of soils can be very low, often below 5%. Therefore the relative contribution of contaminants can be considerable. The organic content of the sample can be as follows:

1. Autochthonous carbon, formed during deposition; this is generally the datable fraction;
2. Allochthonous carbon, which was part of the deposited matrix prior to the formation of the autochthonous carbon; this carbon causes older ages;
3. Reworked or eroded allochthonous organic matter, usually older, which is redeposited in the dated layer;
4. Younger carbon from stratigraphically lower depths, like fulvic and humic acids;
5. Rootlets from higher, younger levels.

After the removal of roots and coarse sands by sieving (physical pretreatment), soil samples undergo chemical pretreatment to isolate the datable fraction and to remove contaminants (Mook and Streurman, 1983).

Based on their solubilities, the organic compounds are generally subdivided into fulvic acids (soluble in alkaline and in acids) and humic acids (soluble in alkaline, precipitating in acids). A residual fraction (often referred to as humin) is insoluble in both acids and alkaline. The latter organic molecules, originating from the decomposition of organic matter, are relatively resistant against further degradation. This humin fraction is therefore considered the allochthonous organic matter.

Fulvic acids represent a very unstable phase of humic components, which is highly mobile and moves relatively quickly through a profile. Since in general there is net water transport downward, this means that they usually show a younger age than other fractions at the same depth. Nevertheless, for soils, humic acid is the most reliable datable fraction.

Generally, a consistent date for both humin and alkaline fraction (the humic acid) is a quality check for the homogeneity of the sample. This is then considered as a good indication of the relative integrity of the material selected for dating.

A schematic illustration of the pretreatment is shown in Fig. 3.1.3. For the datable fraction (the humic acid) the carbon content C_v is about 60% for good quality samples (C_v is defined later; see also Mook and Streurman, 1983).

3.1.7 Reservoir effects

The ^{14}C convention is defined for terrestrial material, which is in equilibrium with atmospheric CO_2. Reservoirs like oceans, rivers and

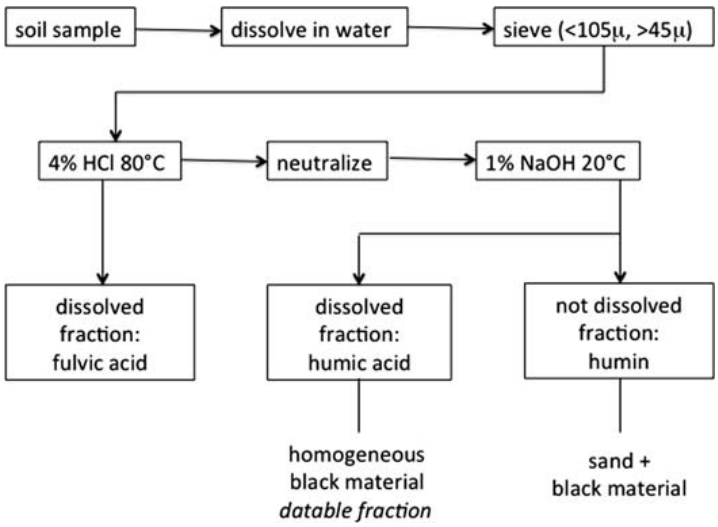

FIGURE 3.1.3 Scheme for pretreatment of soil samples for ^{14}C dating.

lakes generally contain less ^{14}C than the atmosphere. This causes apparent ages for organisms acquiring their carbon from these reservoirs: the so-called 'reservoir effect'.

For the marine reservoir, the size of this effect is 400 years. The activity of the ^{14}C standard can be taken as $^{14}a^0 = 100\%$, representing the activity of modern atmospheric material (Mook and van der Plicht, 1999). A difference of 400 years corresponds to 5% in activity, so that modern marine plants show a recent activity of 5% less than the standard (thus their $^{14}a^0 = 95\%$).

For non-marine aquatic reservoirs the size of the effect depends on the chemical/physical conditions. Obviously, for the purpose of ^{14}C dating, knowledge of the size of the reservoir effect is essential. For plant material that forms the constituent of soil organic matter, the stable isotope value $\delta^{13}C$ can be used to obtain information on the reservoir effect for ^{14}C.

For example, submerged plants show typical $\delta^{13}C$ values of about $-38‰$ in running water, and between -22 and $-15‰$ for stagnant water. These $\delta^{13}C$ values correspond to recent activities of $^{14}a^0 = 85\%$ and 100%, respectively. This in turn corresponds to reservoir effects of 1300 and 0 years, respectively (van der Plicht et al., 2001/2002; Olsson, 1983). The number 85% is generally valid for the Holocene but for the (Late) Glacial it can be much lower (Meadows, 2005).

3.1.8 Carbon isotopes in different types of deposits

We briefly summarize here various types of soil, with characteristic values for the carbon isotopes: $\delta^{13}C$ and $^{14}a^0$. This is based on laboratory experience based on many dating projects during the last six decades.

Gyttjas show typical $\delta^{13}C$ values of $-15‰$ (stagnant) and $-38‰$ (running); for $^{14}a^0$ this corresponds to 100% and 85%, respectively. The latter leads to a significant reservoir effect.

Lake sediments show typical $\delta^{13}C$ values between -22 and $15‰$ and $-38‰$. Because this concerns submerged aquatic plants, ^{14}C dates do show reservoir effects.

Soils show typical $\delta^{13}C$ values between $-26‰$ (from vegetation living under dry conditions) and $-30‰$ (from vegetation living under wet conditions). Sometimes inversion of ^{14}C dates is observed, depending on the amount of allochthonous carbon in the soil and the dry/wet conditions during soil formation, as well as on redeposition of organic material. Usually, there are no reservoir effects (no aquatic plant material is involved).

Note also that redeposition itself plays an important role in the aberrant ^{14}C dates obtained for (micro)podzols.

Vegetation horizons do not show reservoir effects or inversions of ^{14}C dates; some redeposition is possible. The $\delta^{13}C$ values are typically -25 to $-27‰$.

Coastal peat does not show significant reservoir effects or inversion of ^{14}C dates. The $\delta^{13}C$ values are typically between -26 and $-30‰$.

Peat bogs show hummocks ('horsten') or hollows ('slenken'), depending on dry or wet zones in the bog.

The driest conditions result in $\delta^{13}C$ values around $-28‰$. There are no reservoir effects.

The wettest conditions result in $\delta^{13}C$ values around $-19‰$. In this case, reservoir effects are possible by bacterial methanogenesis. Methane (CH_4) is very depleted in ^{13}C ($\delta^{13}C \approx -70‰$); the $\delta^{13}C$ of the resulting CO_2 can be as high as $\delta^{13}C = +10‰$. The $\delta^{13}C$ value of atmospheric CO_2 is about $-7‰$; mixing with $+10‰$ obviously results in higher $\delta^{13}C$ values after photosynthesis by the plants. This may cause reservoir effects or inversions.

In marine sediments (coastal) in coastal regions there is a mixture between marine and riverine influence. Marine plants have a $\delta^{13}C$ value of $-17‰$; the older river sediments have a $\delta^{13}C$ value of about $-28‰$. The mixed value is then $\delta^{13}C = -22‰$. The mixing ratio

also determines the magnitude of the reservoir effect.

In marine sediments (sea and ocean) there is no influence from rivers, so here only the marine reservoir effect of 400 years applies.

3.2 Radiocarbon dating of polycyclic soil sequences in Late Glacial and Holocene aeolian sand deposits (profile Weerterbergen, southeast Netherlands)

3.2.1 Introduction

The landscape of Weerterbergen between the cities of Weert and Budel (southeast Netherlands) is an example of an inland dune landscape in the Pleistocene coversand district. Coversand is chemically poor medium fine aeolian sand deposited in the Weichselian Late Glacial and dominates the surface geology of an extensive part of northwest Europe (Castel et al., 1989; van Mourik et al., 2012a,b).

During the Preboreal the area stabilized under a pioneer vegetation, consisting of herbal species, and the first phase of foil formation was an Umbrisol. After the Preboreal, warmer and moist climatic conditions promoted the development of forests and in the course of the Boreal and Atlantic, a deciduous forest covered the area and the soils evolved to umbric Podzols.

In prehistoric and early historical times, forest grazing, wood cutting and shifting cultivation gradually transformed the forest into heath. Subsequently, the use of the heath for the production of sheep manure during the period of plaggic agriculture (from the early Middle Ages to the introduction of chemical fertilizers around AD 1900), but especially commercial deforestations during the 11th–14th centuries, resulted in the local remobilization of coversands and led to major phases of sand drifting (Vera, 2011). Locally, the coversand landscape transformed into a driftsand landscape with characteristic new landforms and soils (van Mourik, 1988, 2012a,b).

Interesting soil archives in these cultural landscapes are polycyclic driftsand sequences, geoecological records of a succession of cycles of alternating unstable and stable phases in landscape development. As a representative example we present the results of profile Defensiedijk-1, one of the most complete soil archives of driftsand landscapes in the southeast Netherlands situated in the Weerterbergen (Fig. 3.2.1). The sequence consists of three complete geomorphological cycles. The profile is shown in Fig. 3.2.2.

Soil pollen analysis provides information as to whether such alternating periods of landscape stability and instability were caused by changing climatic conditions or by land use. But soil archives also need to have their chronology established by absolute dating. Traditionally, radiocarbon dating of soil organic matter extracted from buried humic (Ah) horizons was used to date individual cycles of the polycyclic sequence. However, this approach has two disadvantages.

First, extracted soil organic matter from buried humic horizons has a complicated composition in terms of chemical characteristics and ages (Goh and Molloy, 1978; Ellis and Matthews, 1984; Stevenson, 1985). This must be considered when interpreting the ^{14}C results.

Second, every geomorphological cycle reflects a period of landscape instability (sand drifting) and landscape stability (soil development). The ^{14}C ages of buried soil horizons identify aeolian deposition phases, but they do not separate within one cycle the time used for sand deposition and time available for soil formation.

The interpretation of the radiocarbon dates of the 'bulk' samples of the buried Ah horizons was problematic. Therefore we decided to resample the buried Ah and Bh horizons to perform fractionated dating to evaluate the reliability of radiocarbon dating of such soil archives (van Mourik et al., 1995).

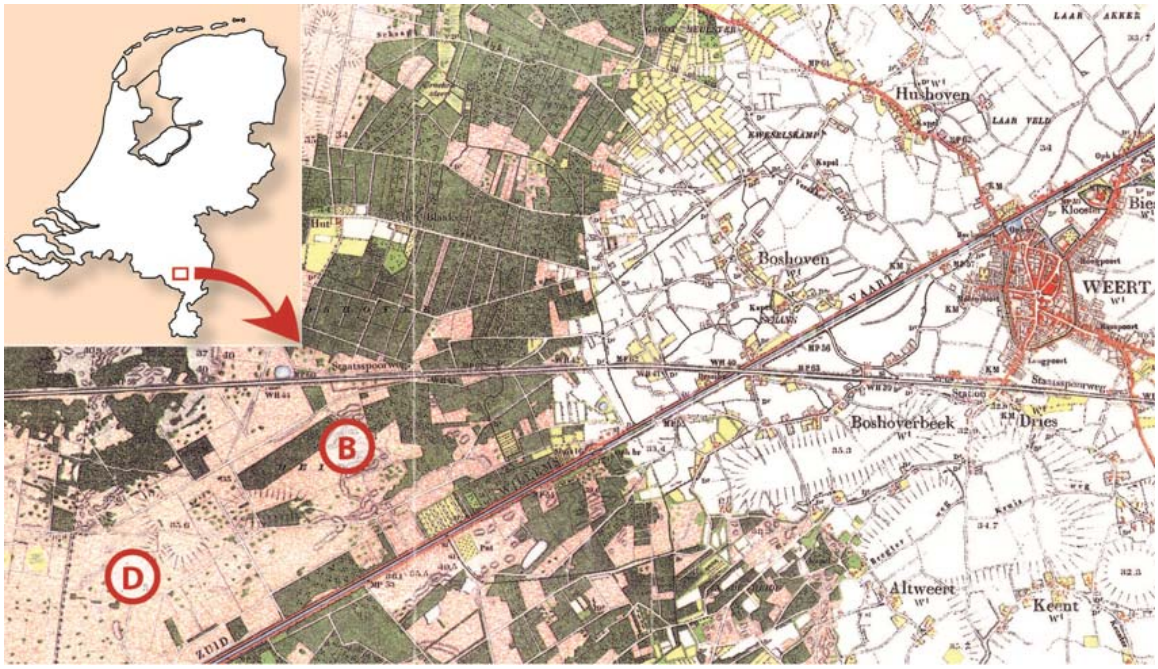

FIGURE 3.2.1 Part of the historical topographical map (scale 1:25.000) showing the location of the profiles Defensiedijk-1 (D) and Boshoverheide-1 (B). The map shows the landscape around the city of Weert in 1901 AD with the distribution of arable fields (*white*), heath and driftsand (*pink*) and the first reforestation with Scotch Pine (*green*). *After van Mourik, J.M., Seijmonsbergen, A.C., Jansen, B., 2012a. Geochronology of Soils and Landforms in Cultural Landscapes on Aeolian Sandy Substrates, Based on Radiocarbon and Optically Stimulated Luminescence Dating (Weert, SE-Netherlands). Intech Radiometric dating, 75–114; van Mourik, J.M., Seijmonsbergen, A.C., Slotboom, R.T., Wallinga, J., 2012b. The impact of human land use on soils and landforms in cultural landscapes on aeolian sandy substrates (Maashorst, SE Netherlands). Quaternary International 265, 74–89.*

The pollen diagram for Defensiedijk-1 (Fig. 3.2.3) shows a record of several cycles in landscape development. The technique of pollen extraction and determination is according to Moore et al. (1991). Based on the pollen density curve (log *D*) it is possible to recognize periods with sand deposition (with a syn-sedimentary pollen content) and periods with soil formation (with a post-sedimentary pollen content). The unstable phases with sand drifting and deposition are indicated with the code D (2D, 3D, 4D, 5D). Phase 1D concerns Late Weichselian coversand; this sediment is palynologically sterile and not registered in the pollen record. The stable phases with soil formation are indicated with the code S (1S, 2S, 3S, 4S).

The pollen spectra of cycle 1S show high percentages of deciduous trees, mainly *Corylus*, *Alnus* and *Quercus*; the percentages of Ericaceae are increasing. Pollen infiltration took place from the beginning of the Preboreal until burial around 3615 BP. Consequently, the older pollen spectra do not show a record of the vegetation development from 9000 to 3600 BP, because the older pollen content is continuously erased by younger pollen. But pollen spectra with high percentages of *Corylus* and *Quercus* and upcoming heath are indicative for the Bronze Age and early Iron Age, which is consistent with the radiocarbon age of the HAC fraction of the 4Ah horizon (3615 BP). At that time, soil formation in coversand reached the stage of carbic Podzol.

FIGURE 3.2.2 Picture of profile Defensiedijk-1, sampled in 1984.

Cycle 2 starts with deposition of the pre-Medieval driftsand (D2). The pollen densities are low; the pollen content is syn-sedimentary. There is a slight increase of Poaceae, indicating some degradation of heath in the surroundings. Zone 2S shows the vertical distribution, indicative for pollen infiltration during the formation of the carbic Podzol. The spectra are dominated by Ericaceae. The ^{14}C date of the humic acids fraction of the 3Ah (1365 BP) is pre-Medieval.

Cycle 3 starts with the deposition of Medieval driftsand (D3). The sedimentary pollen concentrations of the driftsand layers indicate a relatively low sedimentation rate. The pollen spectra are still dominated by Ericaceae, but Poaceae are rising, pointing to increasing degradation of the heath. During the next stable period (3S), an initial Podzol (micro-Podzol) developed. The 2A horizon of the micro-Podzol shows pollen spectra with increasing percentages of *Pinus*. Reforestation with pine trees to stabilize driftsand landscapes started in the Netherlands after AD 1550. This is consistent with the ^{14}C date of the humic acid fraction (410 BP) of the 2Ah horizon.

Cycle 4 starts with the sedimentation of the post-Medieval driftsand (D4). Since 1995 the area stabilized under a vegetation of grasses and lichens. This stable period is too short for soil formation and is in the initial phase of a Rhizomull humus form.

Based on radiocarbon dates of humic acid fractions of buried Ah horizons we can make a distinction in three periods characterized by instability and sand drifting: pre-Medieval, Medieval and post-Medieval. In the next paragraph we explain why dates of the humic acids fractions instead of the bulk samples are used.

Based on the pollen diagram we can conclude that there are no palynological indications that climatic change was responsible for unstable periods with sand drifting. Human influence, forest degradation and heath management seem to be the dominant factors.

3.2.2 Fractionated radiocarbon dating of profile Defensiedijk-1

The results of the radiocarbon dating of bulk samples of the three buried Ah horizons collected in 1984 were not reliable for establishing the chronology of the cycles. Especially, the dating of the 2H2 horizon was 'too old'. Therefore we resampled the profile in 1986 for fractionated radiocarbon dating. The results are shown in Table 3.2.1.

Some micrographs (terminology based on Brewer, 1976) are shown to illustrate complications in the composition of organic matter in soils (Figs. 3.2.4–3.2.9).

For each sample (with the exception of the bulk samples), three chemical fractions were

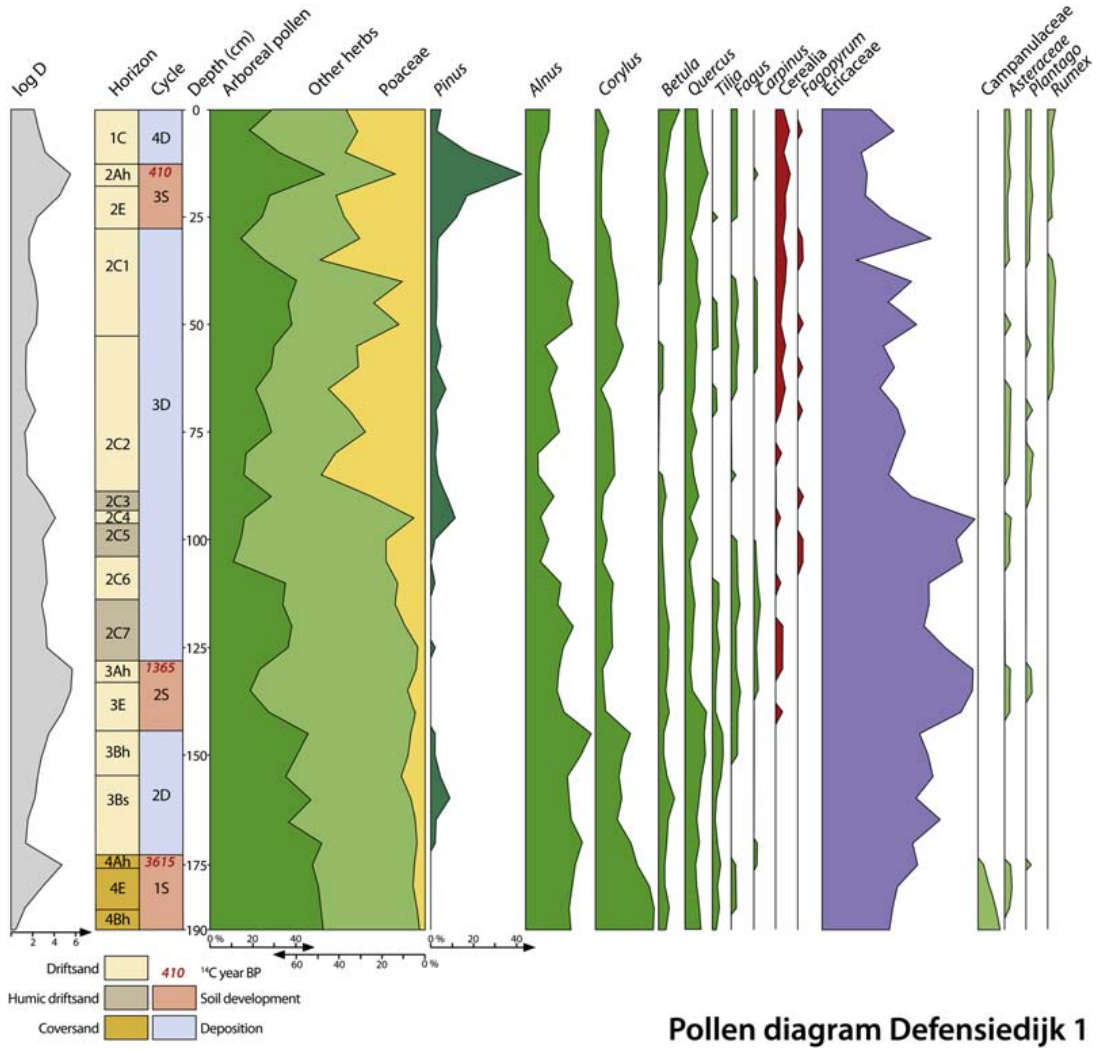

FIGURE 3.2.3 Pollen diagram Defensiedijk-1. The ^{14}C dates are based on the humic acid fraction of the buried Ah horizons. *After van Mourik, J.M., Seijmonsbergen, A.C., Jansen, B., 2012a. Geochronology of Soils and Landforms in Cultural Landscapes on Aeolian Sandy Substrates, Based on Radiocarbon and Optically Stimulated Luminescence Dating (Weert, SE-Netherlands). Intech Radiometric dating, 75–114; van Mourik, J.M., Seijmonsbergen, A.C., Slotboom, R.T., Wallinga, J., 2012b. The impact of human land use on soils and landforms in cultural landscapes on aeolian sandy substrates (Maashorst, SE Netherlands). Quaternary International 265, 74–89.*

prepared and dated: fulvic acids, humic fraction and residue. For all fractions, the amount of sample (in grams) is shown, as well as the amount of carbon extracted. The C_v is determined as (amount of C)/(amount of sample minus amount of ash) * 100%. The Cpr is the relative amount of carbon after pretreatment; the C_v is the relative amount of the organic fraction (Mook and Streurman, 1983). For each fraction, the ^{14}C age is measured and shown in BP with its 1-sigma measurement uncertainty, as well as the $\delta^{13}C$ value.

TABLE 3.2.1 List of radiocarbon dates and sample compositions of profile Defensiedijk-1.

Lab code	Horizon	Depth (cm)	Fraction	Sample (g)	C (g)	Cpr (%)	Cv (%)	^{14}C age (BP)	Sigma	δ^{13}C (‰)
GrN-12804	2Ah	025–027	Bulk	55.0	1.03	38	53	1130	60	−27.68
GrN-14833			Humin	96.2	0.67	<1	50	3230	110	−27.98
GrN-14458			Humic	3.00	1.43	48	53	410	45	−27.00
GrN-14759			Fulvic	0.95	0.33	35	50	110	110	−26.84
GrN-12805	3Ah	127–129	Bulk	206.0	7.35	29	54	1075	30	−27.78
GrN-14837			Humin	95.8	1.57	2	33	1350	45	−27.19
GrN-14459			Humic	14.5	7.41	51	56	1365	25	−27.31
GrN-14760			Fulvic	1.20	0.43	36	44	850	100	−26.36
GrN-14838	3Ah	129–131	Humin	120.0	0.53	<1	26	1900	110	−28.87
GrN-14694			Humic	8.50	3.43	40	44	1675	30	−27.33
GrN-14774			Fulvic	0.73	0.23	32	41	1200	130	−26.03
GrN-14695	3B2h	147–148	Humin	18.5	9.00	49	54	1820	25	−29.84
GrN-14765			Fulvic	1.29	0.48	37	40	1160	90	−27.45
GrN-14696	3B2h	149–150	Humic	17.0	6.71	39	44	1670	25	−28.70
GrN-14772			Fulvic	1.85	0.65	35	42	1160	70	−27.22
GrN-14843	3B2h	147–150	Humin	256.0	1.00	<1	18	1445	60	−28.62
GrN-14841	3B2h	151–152	Humin	133.5	0.36	<1	14	1900	140	−26.43
GrN-14697			Humic	7.50	3.58	48	54	1700	30	−28.34
GrN-14770			Fulvic	2.35	0.98	42	52	1480	60	−27.50
GrN-12806	4Ah	173–174	Bulk	269	2.71	16	53	3920	40	−29.72
GrN-14836			Humin	133.3	0.75	<1	36	4110	90	−26.27
GrN-14460			Humic	7.30	3.15	48	63	3615	35	−28.02
GrN-14761			Fulvic	1.20	0.25	21	30	2200	170	−27.60
GrN-14840	4Ah	175–176	Humin	137.9	0.50	<1	26	4430	160	−27.94
GrN-14698			Humic	5.20	1.96	38	44	3965	40	−28.34
GrN-14775			Fulvic	1.18	0.36	30	36	3010	140	−27.11
GrN-14699	4B2h	185–186	Humic	9.90	3.18	32	37	3985	35	−27.32
GrN-14768			Fulvic	1.74	0.48	28	40	2900	100	−26.96
GrN-14700	4B2h	187–188	Humic	11.5	3.85	33	38	3730	35	−28.04
GrN-14767			Fulvic	1.91	0.44	23	32	2890	110	−26,58

(*Continued*)

TABLE 3.2.1 List of radiocarbon dates and sample compositions of profile Defensiedijk-1.—cont'd

Lab code	Horizon	Depth (cm)	Fraction	Sample (g)	C (g)	Cpr (%)	Cv (%)	^{14}C age (BP)	Sigma	δ^{13}C (‰)
GrN-14701	4B2h	189–190	Humic	10.7	4.00	37	44	3700	50	−26.10
GrN-14766			Fulvic	2.37	0.96	40	40	2830	110	−27.01
GrN-14849	4B2h	185–190	Humin	395.0	0.80	<1	14	3550	80	−27.59

Cpr, relative amount of carbon after pretreatment; *Cv*, (amount of C)/(amount of sample minus amount of ash) * 100%.

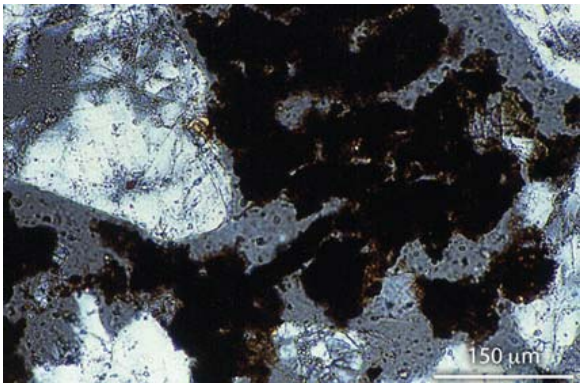

FIGURE 3.2.4 Micrograph of intertextic distributed organic aggregates (3Ah horizon).

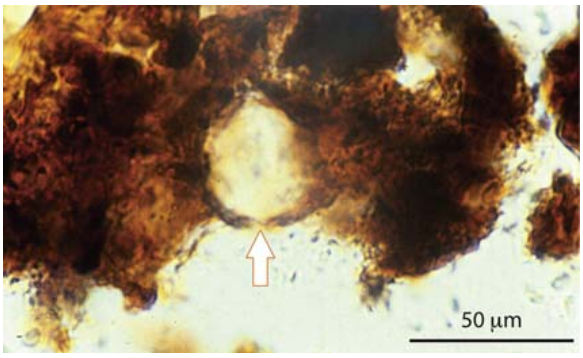

FIGURE 3.2.5 Micrograph of the internal fabric of an intertextic aggregate (in the centre is an embedded pollen grain).

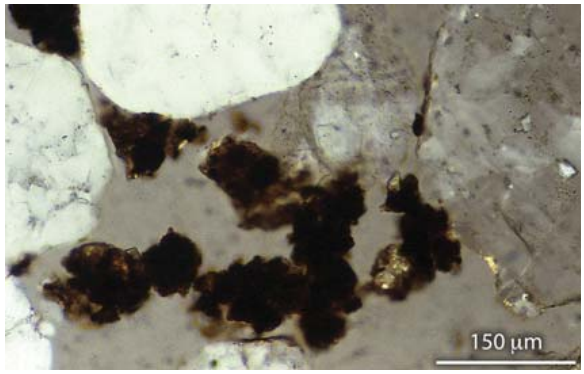

FIGURE 3.2.6 Micrograph of a root hole with (down-moving) organic aggregates in the 3E horizon.

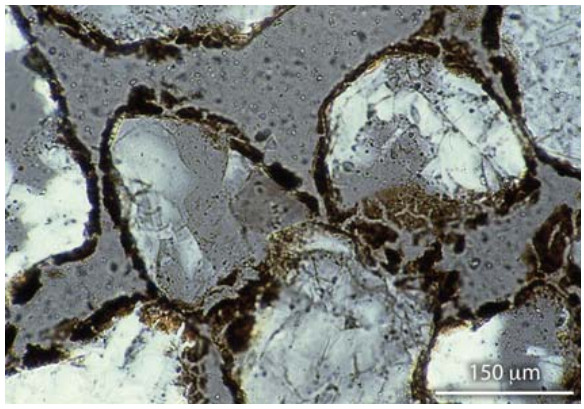

FIGURE 3.2.7 Micrograph of organic cutans in the 3Bh horizon.

As explained earlier, fulvic acids represent the mobile fraction, humic acid is considered to be the datable fraction and the humin fraction contains the older material. When the dates of humic acid and the humin fraction are the same within mutual uncertainty, the ^{14}C date can be considered reliable. An example is sample 3Ah (127–129 cm depth).

As can be seen from Table 3.2.1, fulvic acids are much younger than the other fractions. This

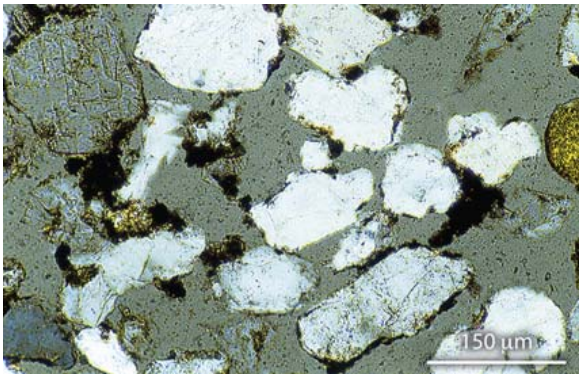

FIGURE 3.2.8 Micrograph of organic particles (including charcoal) in the 2C horizon.

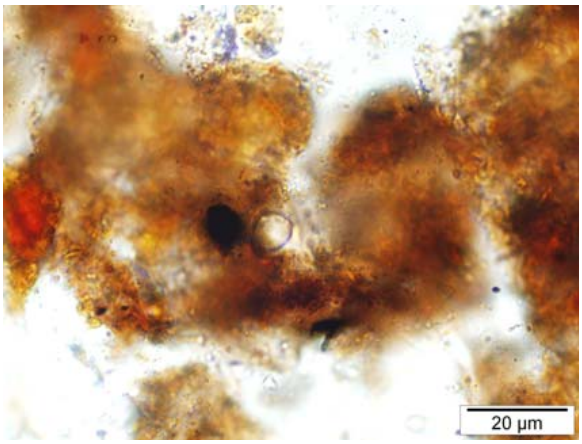

FIGURE 3.2.9 Micrograph of the internal fabric of welded aggregates (including pollen and charcoal) in the 2A horizon.

shows that this fraction is not the correct ^{14}C datable material. The humic fraction shows a more or less reliable stratigraphy for this soil sequence. Radiocarbon dates of other polycyclic profiles with similar results have been published in van Mourik et al. (2012a,b).

The general conclusion is that the humic acid fractions are the best datable fractions for ^{14}C, as expected. The stratigraphic order is correct. There is no significant inversion. Only GrN-14695 shows a very negative $\delta^{13}C$ value. This can be an indication of wetter conditions at the time of soil formation, resulting in a change in type of vegetation.

3.2.3 Radiocarbon dating of Boshoverheide

A second polycyclic profile Boshoverheide-1 was sampled in a small plateau dune, 1750 m northeast of profile Defensiedijk-1 (Figs. 3.2.10 and 3.2.11). The pollen diagram is shown in Fig. 3.2.12, and the dates in Table 3.2.2.

In this profile the cycle of deposition and podzolation in pre-Medieval driftsand is missing. Pre-Medieval drift deposits are very local small-scale features and the result of natural events such as storms and forest fires, and cultural degradation by shifting cultivation (van Mourik, 1988). Other cycles related to regional Medieval and post-Medieval sand drifting are recorded. The pollen zoning of Boshoverheide-1 (Fig. 3.2.12) and the series of radiocarbon dates show similar trends to profile Defensiedijk-1 (Table 3.2.1).

The palynological age (dominance of *Alnus* instead of *Corylus*) and the ^{14}C dates of the buried Podzol, developed in coversand, point to a Middle Subatlantic age. This means that the development of the carbic Podzol of the

FIGURE 3.2.10 Small plateau dune on the Boshoverheide.

FIGURE 3.2.11 Profile Boshoverheide-1.

oldest cycle (1S) was continuous from the deposition of coversand (Late Glacial/Preboreal) until about AD 1200.

The burial of the Palaeopodzol by Medieval driftsand took place after AD 1200. This is still consistent with the period of forest clearing as reported by Vera (2011).

Cycle 2S in profile Boshoverheide-1 was included in a study of initial Podzols in the Weerterbergen to answer the question whether these initial Podzols (Mormoders) were indicative for a regional or only a local phase of landscape stability by applying both ^{14}C and optically stimulated luminescence (OSL) dating (Wallinga et al., 2013). The sampling strategy is shown in Fig. 3.2.13; the OSL dates from the top of 2C and the bottom of 1C are presented in Table 3.2.2.

The time available for the development of the initial Podzol (2S), representing the stable phase with soil formation between the depositions of D2 and D3, was less than 150 years (based on OSL dates). The radiocarbon ages of the carbon fractions extracted from the 2AE appear too old. The OSL age of the base of the C horizon (driftsand and phase D3) fits with the second regional extension of sand drifting related to the overexploitation of the heaths during the 18th century.

Parts of the soil organic matter of Holocene driftsand deposits (the parent material for soil development) are eroded and transported (older) organic particles of former vegetation layers, grains with organic cutans originating from Podzols eroded elsewhere and charcoal fragments affecting the results of the ^{14}C dating (Figs. 3.2.14 and 3.2.15).

Since the Late Neolithic, people occupied the landscape and caused degradation of vegetation and soil. The oldest relics in the Weerterbergen are small-scale sand drifts, related to shifting cultivation as recorded in the Defensiedijk profiles. A second group of relics are barrows from the Bronze Age and Iron Age. More degradation and extensive sand drifts were caused by deforestations in the 11th–13th centuries and the overexploitation of the heaths in the 18th century.

The Boshoverheide is nowadays an archaeological reserve containing several restored barrows. Fig. 3.2.16 shows a barrow close to the investigated profile of Boshoverheide-1. The profile is shown in Fig. 3.2.17. The ^{14}C dating of a bulk sample of the buried Ah horizon (GrN-13515, 2400 ± 60 BP) and the palynological age of the 2Ah Podzol buried by the barrow fit with 1S of Boshoverheide-1 (van Mourik, 1988). The ^{14}C dates of the 2Ah horizons below five other barrows range from 2460 to 2610 BP (Groenman-van Waateringe, 1988). Consequently, the pre-Medieval driftsands of Defensiedijk-1, the Medieval sand dune of Boshoverheide-1 and the barrows on

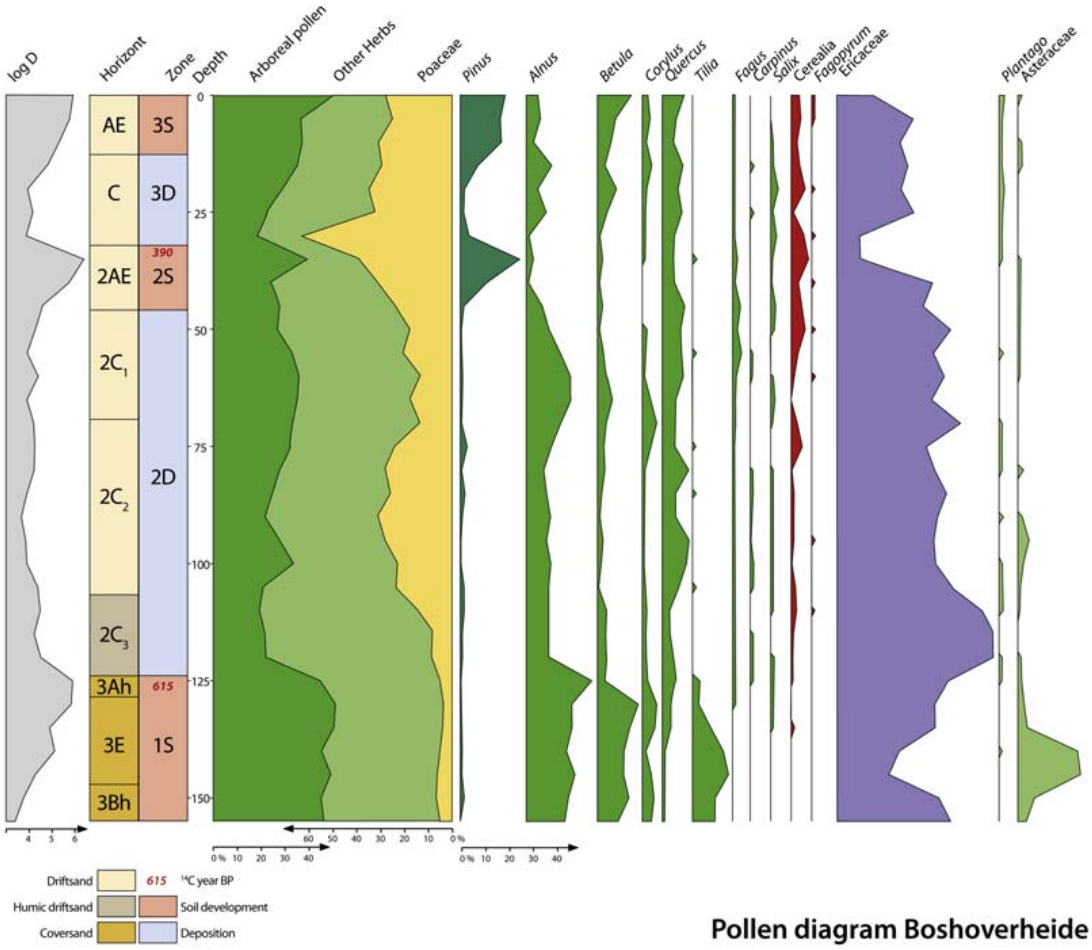

FIGURE 3.2.12 Pollen diagram Boshoverheide-1.

the Boshoverheide came into existence on the same surface, a podzolic soil, developed in coversand. Podzolation could continue until burial by pre-Medieval driftsand covers, barrows, Medieval and post-Medieval driftsand covers and land dunes. The accuracy of the dating methods determines the details of our knowledge of the geochronology of these relics.

The next step in the study of the geochronology of sequences of aeolian sand deposits was the application of luminescence dating of mineral grains (Chapter 4). In 1989 the Aberystwyth Luminescence Research Laboratory was founded and a promising technique (thermoluminescence (TL) dating) became available for the dating of sandy deposits. As a pilot, the sand deposits of the cycles of profile Defensiedijk-1 were resampled for TL application.

Every geomorphological cycle started with an unstable period with sand deposition, followed by a stable period with soil formation. The research question was whether we could determine the duration of the unstable periods and the remaining time for soil

TABLE 3.2.2 ^{14}C and OSL dating of profile Boshoverheide-1.

Number	Horizon	Depth (cm)	Fraction	^{14}C age (BP)	Calibrated ^{14}C age (AD)	$\delta^{13}C$ (‰)	OSL age (AD)
NCL 5106010	1C	027–032	Quartz				1957 ± 3
GrN-12869	2AE	033–035	Bulk	265 ± 30	1539 ± 58		
GrN-14834	2AE		Humin	1710 ± 35	321 ± 53	−26.87	
GrN-14461	2AE		Humic acids	390 ± 25	1521 ± 67	−26.90	
GrN-14762	2AE		Fulvic acids	240 ± 80	1694 ± 125	−26.77	
NCL 5106011	2C	035–040	Quartz				1810 ± 9
GrN-12870	3A	125–127	Bulk	1190 ± 30	829 ± 42	–	
GrN-14835	3A		Humin	830 ± 60	1172 ± 70	−28.49	
GrN-14462	3A		Humic acids	615 + 45	1344 ± 40	−28.04	
GrN-14763	3A		Fulvic acids	490 ± 70	1410 ± 68	−27.30	
GrN-14839	3A	127–129	Humin	1460 ± 90	556 ± 85	−26.59	
GrN-14702	3A		Humic acids	840 ± 45	1182 ± 52	−27.68	
GrN-14773	3A		Fulvic acids	835 ± 55	1172 ± 67	−27.62	
GrN-14703	3Bh	148–149	Humic acids	1100 + 45	935 ± 44	−28.62	
GrN-14771	3Bh		Fulvic acids	910 + 70	1118 ± 71	−27.03	
GrN-14704	3Bh	150–153	Humic acids	1230 ± 70	790 ± 82	−26.88	
GrN-14769	3Bh		Fulvic acids	1020 + 60	1026 ± 76	−26.83	
GrN-14705	3Bh	152–190	Humic acids	1115 + 35	908 ± 37	−28.12	
GrN-14764	3Bh		Fulvic acids	1058 + 45	960 ± 47	26.90	
GrN-14845	3Bh	148–153	Humin	1235 ± 85	792 ± 91	−27.61	

formation, which was not possible using radiocarbon dating alone. It was worthwhile approaching this question with TL dating. The TL dates were published by Dijkmans et al. (1992).

The results are presented in Table 3.2.3. In 1993 the luminescence dating laboratory of the University of Ghent was established, and in 2002 profile Defensiedijk-2 was resampled, now for a pilot of the application of OSL dating of coversand and driftsand (van Mourik et al., 2010).

Table 3.2.3 shows the results of the TL and OSL dating of deposits and the ^{14}C dates of the humic acids of the buried Ah horizons. The ^{14}C dates are also calibrated; the results are shown at the 1-sigma confidence level. The TL and OSL dates of 1C, 2C and 4C correspond reasonably well with each other, but the TL ages of 3E are significantly younger than the OSL age. Also, the duration of the phases with soil formation between the phases with sand depositions are not really similar. Especially, the ^{14}C date of 4Ah is too old compared to the OSL date.

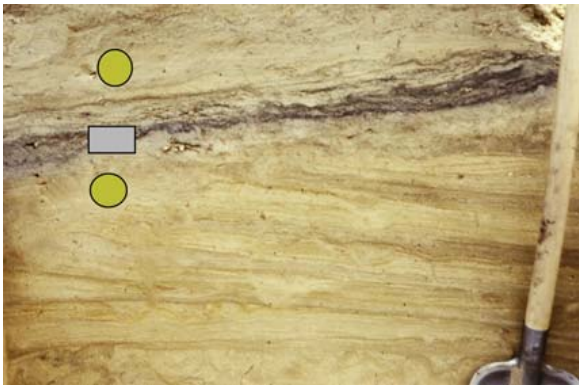

FIGURE 3.2.13 Photograph of the initial Podzol (2AE) in profile Boshoverheide-1 with the sample locations for optically stimulated luminescence dating (*yellow rings*), micromorphology and ^{14}C dating (*grey box*).

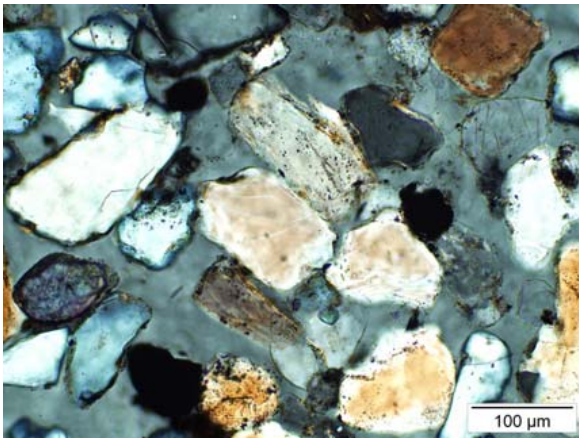

FIGURE 3.2.14 Micrograph of the 2AE horizon (Boshoverheide-1) showing charcoal and organic cutans, originating from elsewhere-eroded Podzols.

The interpretation of dates requires detailed knowledge of processes during active soil formation or sand deposition, but also of the processes after the burial of soils.

Fig. 3.2.18 shows bioturbation (by soil animals or in root holes) that can pollute mineral samples with grains with a younger (downward transport) or older (upward transport) signal. Decomposing roots cause rejuvenation of soil organic matter.

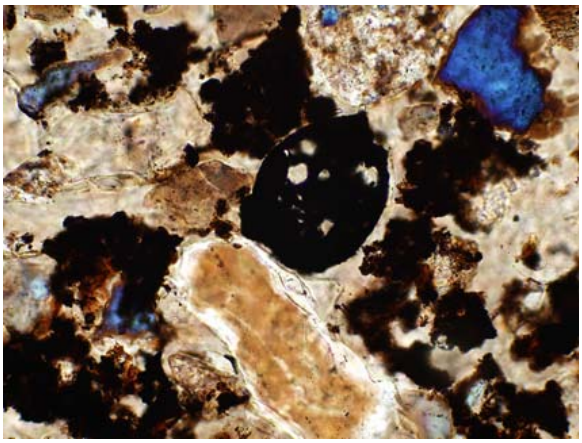

FIGURE 3.2.15 Micrograph of the 2AE horizon (Boshoverheide-1) with (rounded) organic aggregates and charcoal particles.

FIGURE 3.2.16 View of the examined barrow on the Boshoverheide.

FIGURE 3.2.17 Soil profile of the barrow and the buried palaeosol.

TABLE 3.2.3 TL, OSL and ^{14}C dating of the polycyclic sequence Defensiedijk-1.

	(Aberystwyth)	(Gent)	(Groningen)	
Sample	TL age (ka) (feldspar fraction)	OSL age (ka) (quartz fraction)	^{14}C age BP (humic acid fraction)	Calibrated ^{14}C age (calBP)
1C top		0.08 ± 0.01		
1C middle		0.10 ± 0.01		
1C bottom	0.2 ± 0.1	0.09 ± 0.01		
2AE			410 ± 45	335–515
2C top	0.8 ± 0.2	0.59 ± 0.05		
2C middle	0.4 ± 0.2	0.67 ± 0.06		
2C bottom		1.3 ± 0.1		
3Ah			1675 ± 30	1545–1610
3 EC top	3.1 ± 0.3	5.8 ± 0.5		
3 EC bottom	3.1 ± 0.3	4.7 ± 0.4		
4Ah			3615 ± 35	3880–3975
4C top	7.7 ± 0.6	9.2 ± 0.8		
4C (bottom)	9.6 ± 0.8			

FIGURE 3.2.18 Detail of the deepest buried Podzol of profile Defensiedijk-1, showing evidence of (palaeo)bioturbation through the 3Ah horizon (profile 1984).

3.3 Absolute and relative dating of the Gasserplatz soil archives (Vorarlberg, Austria) and the reservoir effect

3.3.1 Introduction

The Late Glacial is a period of rapid climate change that marks the transition from the last Glacial to the Holocene. It can be subdivided into stadial and interstadial phases, which were clearly recognized in the Greenland ice core records (Johnsen et al., 2001). These changes in climate are also recognized in pollen diagrams of Late Glacial deposits on the Gasserplatz (Austria, Vorarlberg).

Gasserplatz is a shallow basin in the rather flat confluence area of the former glaciers of the rivers Rhine and Ill (Simons, 1985;

de Graaff et al., 1989). This area became ice free during the Feldkirch stadium (around 15,500 calBP) and developed as a tiny ice-marginal lake in a sheltered position at an elevation of 559 m above sea level. During the Late Glacial, lacustrine carbonate (calcareous gyttja) with some interbedded initial Histosols was deposited in the accumulated Holocene peat. To deduce information about Late Glacial environmental oscillations, pollen analysis, radiocarbon dating and isotope analyses have been applied to the Late Glacial lacustrine carbonates.

The Gasserplatz sampling site is indicated on the geomorphological map of the area (Fig. 3.3.1). The first sediment core was taken in 1989 with a Dachnowsky sampler from the surface down to 510 cm. Samples from depths of 300–465 cm (vertical sampling distance 2 cm) have been used for pollen and isotope analysis and radiocarbon dating (Gasserplatz-1).

The second core was taken in 2002 very close to the first site using a mechanical auger from the surface down to a depth of 590 cm (Fig. 3.3.2). Samples from depths of 330–530 cm (vertical sampling distance 2 cm) have been used for extractions for (absolute) pollen and isotope analysis (Gasserplatz-2). Also, thin sections have been produced to observe the presence of Laacher See Tephra (LST) (Riede, 2008) and to assess the quality of the limnic carbonates and the initial Histosols (Figs. 3.3.3–3.3.8).

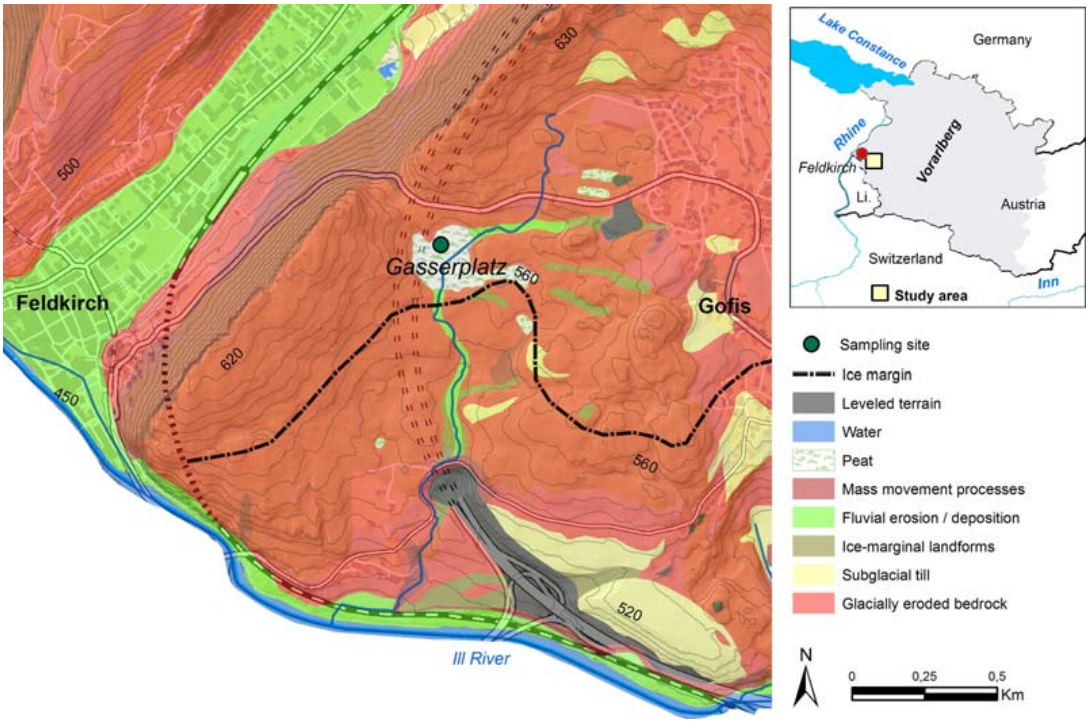

FIGURE 3.3.1 Geomorphological map of the Gasserplatz with the location of the sample site. *After van Mourik, J.M., Slotboom, R.T., van der Plicht, J., Streurman, H.J., Kuijper, W.J., Hoek, W.Z., de Graaff, L.W.S., 2013. Geochronology of Betula extensions in pollen diagrams of Alpine Late-glacial lake deposits: a case study of the Late-glacial deposits of the Gasserplatz soil archives (Vorarlberg, Austria). Quaternary International 306, 3–13.*

FIGURE 3.3.2 Picture of the Gasserplatz with the mechanical auger (March 2002).

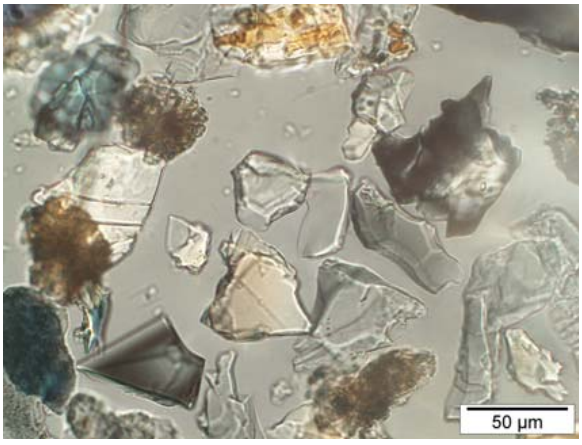

FIGURE 3.3.3 Gasserplatz-2, 383 cm; micrograph of extracted tephra shards.

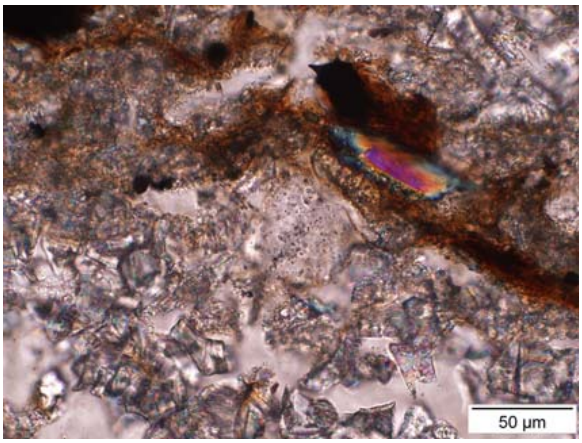

FIGURE 3.3.4 Gasserplatz-2, 383 cm; micrograph of tephra shards in a thin section (*arrow*), deposited in a winter lamella.

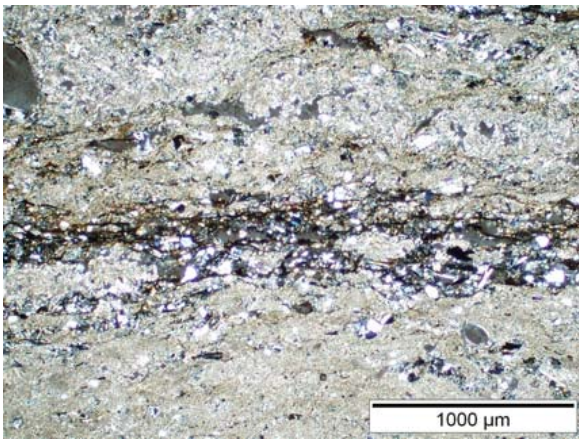

FIGURE 3.3.5 Gasserplatz-2, 505 cm; laminated calcareous gyttja used for ^{14}C dating; light-coloured lamella are winter deposits, rich in organic matter summer deposits. The $\delta^{13}C$ value of the carbonate is $-3.1‰$.

In the Oldest Dryas, lake sedimentation started with clay (glacier milk), followed by the cyclic deposition of calcareous clay and humic calcareous gyttja. The sediment core Gasserplatz-2, sampled with a mechanical auger,

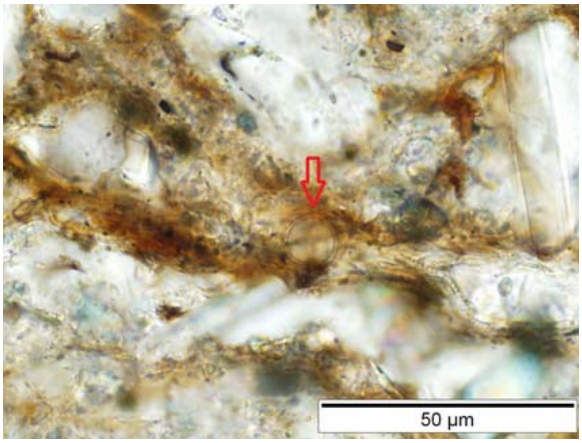

FIGURE 3.3.6 Gasserplatz-2, 505 cm; detail of a humic summer lamella with pollen grain (*arrow*). The $\delta^{13}C$ of the organic fraction is −38.00‰, indicative of biomass produced by aquatic plants.

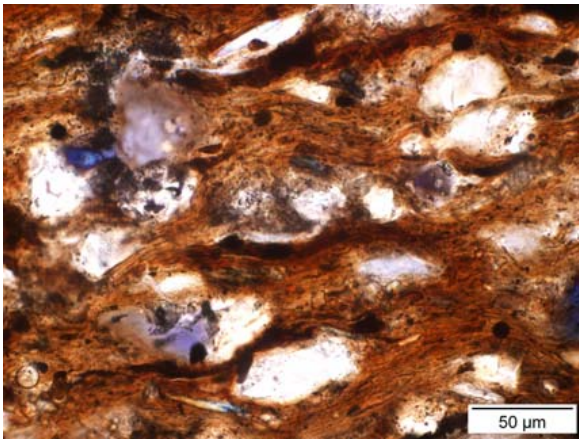

FIGURE 3.3.7 Gasserplatz-2, 386 cm; micrograph of the matrix of the initial Histosols used for ^{14}C dating. The $\delta^{13}C$ value of the peat is −32.4‰, indicative of a mixture of biomass produced by subaqueous and subaerial plants.

allowed the accurate distinguishing of various initial Histosols, a lithological reflection of short-lived periods with relatively low water levels. During the Holocene the lake transferred into a peat bog (Figs. 3.3.9 and 3.3.10).

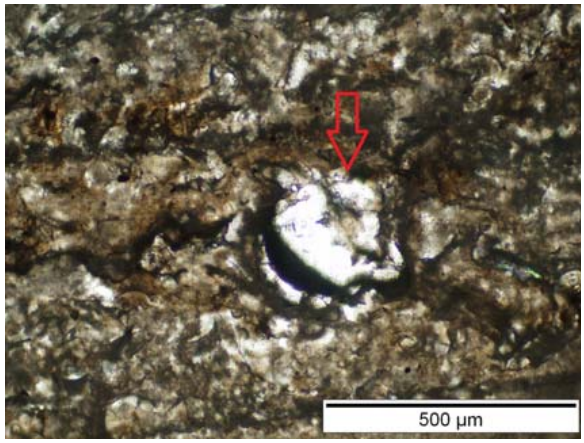

FIGURE 3.3.8 Gasserplatz-2, 468 cm; micrograph of a mollusc in laminated calcareous gyttja used for ^{14}C dating (*arrow*). The $\delta^{13}C$ of a mollusc is around −8.5‰.

3.3.2 Pollen analysis

In the pollen diagrams of Gasserplatz-1 and -2 (previously published in van Mourik et al., 2013), several chronozones can be recognized. They are well expressed in the pollen and isotope stratigraphy and are described next.

Zone I-a, Oldest Dryas. The sedimentation of white laminated calcareous gyttja on sterile blue–grey clay started during the Oldest Dryas. The pollen concentrations of the white gyttja are very low (<200 grains/mL). In the relative pollen diagrams, the Oldest Dryas is dominated by non-arboreal pollen (mainly *Artemisia*, Cyperaceae, *Helianthemum*, Poaceae). The low pollen concentrations indicate that pollen precipitation was mainly the result of long-distance transport. Biomass production in and around the Gasserplatz lake was very low, considering the relatively high $\delta^{13}C$ values.

Zone I-b, Bølling. In the $\delta^{18}O$ curves this interstadial is clearly recognized as a relatively warm period. The deposition of white gyttja with low pollen concentrations continued until a depth of 485 cm. The relative pollen diagrams show a first increase of *Betula* after the

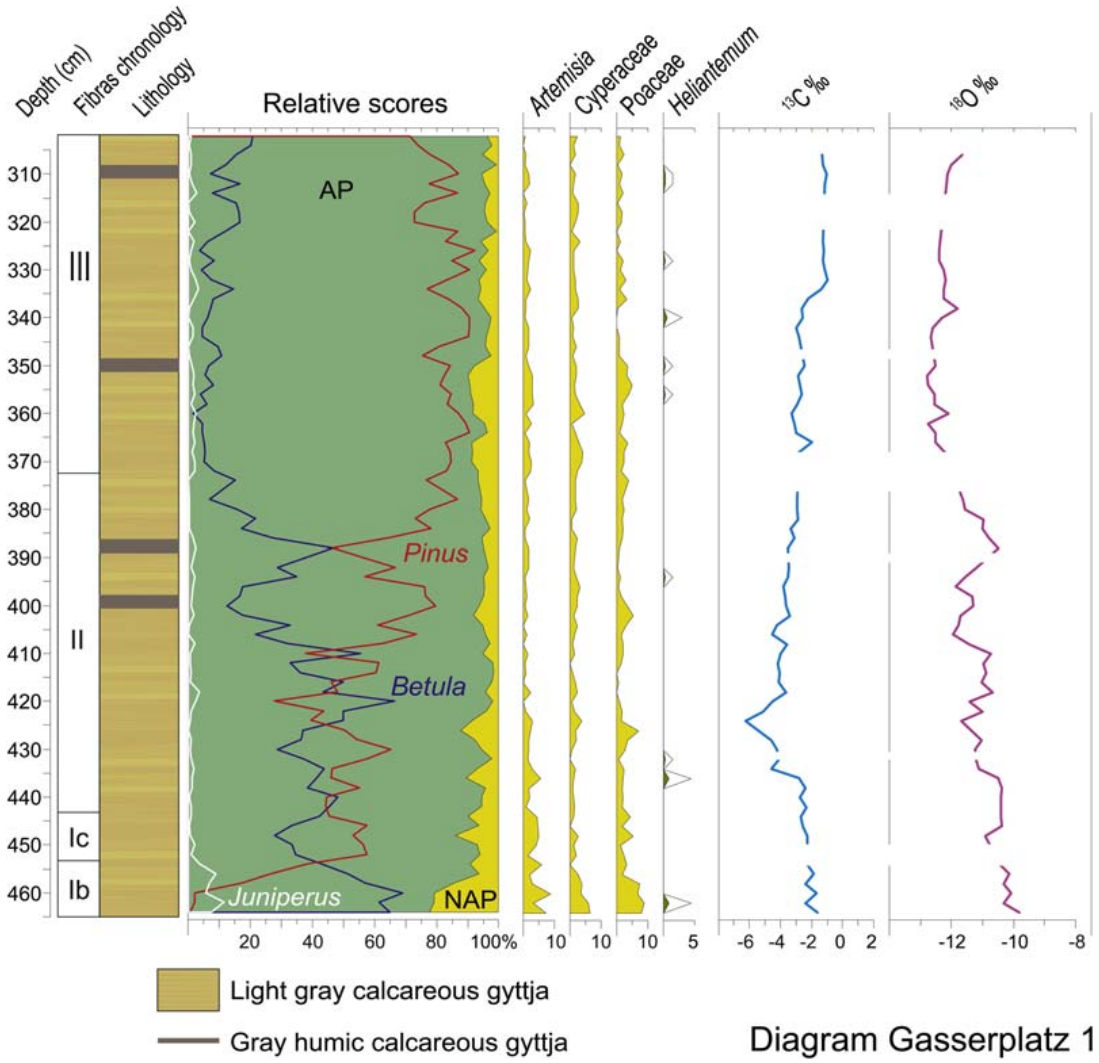

FIGURE 3.3.9 Pollen and isotope diagram Gasserplatz-1, sampled in 1989. *After van Mourik, J.M., Slotboom, R.T., van der Plicht, J., Streurman, H.J., Kuijper, W.J., Hoek, W.Z., de Graaff, L.W.S., 2013. Geochronology of Betula extensions in pollen diagrams of Alpine Late-glacial lake deposits: a case study of the Late-glacial deposits of the Gasserplatz soil archives (Vorarlberg, Austria). Quaternary International 306, 3–13.*

beginning of the Bølling, followed by an expansion of *Juniperus*. The pollen concentration curve of *Betula* provides additional information. Together with the start of deposition of light grey humic gyttja and decreasing $\delta^{13}C$ values from 485 cm, the pollen concentrations increase drastically. This means that the first *Juniperus* arrived in the Gasserplatz area, followed by *Betula* and later by *Pinus*, and started to contribute to local pollen production and dispersion. Consequently, the oldest peak in the relative pollen diagrams must be considered a reflection of a *Betula* expansion on distance; evidently it took time after the deglaciation before *Juniperus*, followed by *Betula* and *Pinus*, first arrived at the Gasserplatz site.

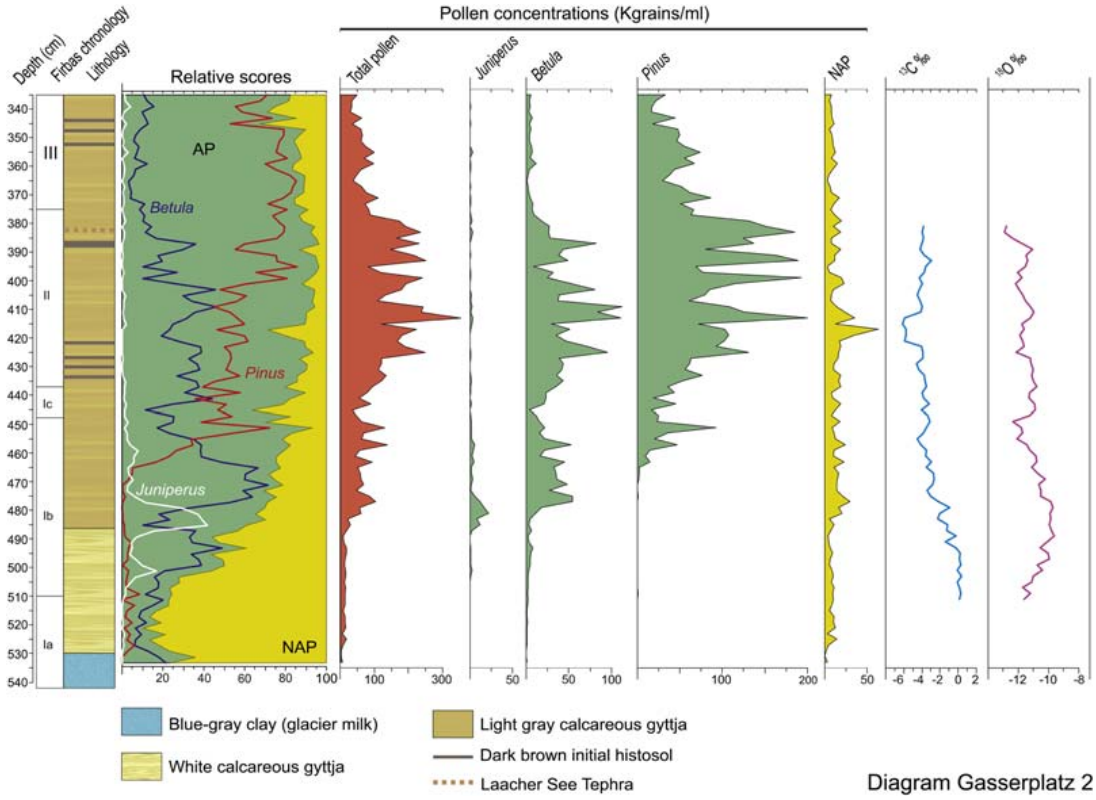

FIGURE 3.3.10 Pollen and isotope diagram Gasserplatz-2, sampled in 2002. *After van Mourik, J.M., Slotboom, R.T., van der Plicht, J., Streurman, H.J., Kuijper, W.J., Hoek, W.Z., de Graaff, L.W.S., 2013. Geochronology of Betula extensions in pollen diagrams of Alpine Late-glacial lake deposits: a case study of the Late-glacial deposits of the Gasserplatz soil archives (Vorarlberg, Austria). Quaternary International 306, 3–13.*

Zone I-c, Older Dryas. This zone is reflected in the diagrams by a decrease in *Betula* and $\delta^{18}O$ as well as an expansion of non-arboreal pollen.

Zone II, Allerød. During the Allerød we can distinguish three oscillations in the *Betula* and $\delta^{18}O$ curves, reflecting three periods with expansion and retreat of *Betula*, likely in reaction to a change in temperature. During these oscillations we observe also a response in the lithology: the deposition of calcareous gyttja is interrupted by the formation of initial Histosols. The characterization of such initial soils was based on a $\delta^{13}C$ value of around −32‰ (Table 3.3.1), suggesting a combination of subaqueous and subaerial conditions.

Zone III, Allerød. During the Allerød, three oscillations in the *Betula* and $\delta^{18}O$ curves are observed, reflecting three periods with expansion and retreat of *Betula*, likely in reaction to a change in temperature. During these oscillations we observe also a response in the lithology: the deposition of calcareous gyttja is interrupted by the formation of initial Histosols. The characterization of such initial soils was based on a $\delta^{13}C$ value of around −32‰ (Table 3.3.1), pointing to a combination of subaqueous and subaerial conditions.

Zone IV, Younger Dryas. During the Younger Dryas, we can distinguish two phases with a short-lived increase in temperature, separating three colder periods, as recorded in the $\delta^{18}O$

TABLE 3.3.1 Results of radiocarbon measurements. GrN: conventional; GrA: AMS.

Lab code	Material	Depth (cm)	^{14}C age (BP)	Sigma (BP)	Calibrated age (calBP)	δ^{13}C (‰)
GrN-32143	Peat	41	1800	60	1820–1630	−28.1
GrN-32144	Peat	65	3370	35	3690–3490	−27.9
GrN-32145	Peat	99	3780	50	4240–4020	−28.8
GrN-15918	Peat	256	8650	70	9675–9540	−27.6
GrN-15919	Peat	283	9500	200	11,125–10,570	−27.8
GrN-31212	Carbonate	309	11,480	100	13,420–13,260	−1.2
GrN-31208	Carbonate	353	11,780	180	13,790–13,440	−2.6
GrN-31206	Carbonate	364	11,920	110	13,890–13,660	−3.1
GrN-31656	Peat	386	11,300	100	13,270–13,120	−32.4
GrA-11476	Snails	468	12,790	70	15,200–15,090	−8.5
GrA-11479	Carbonate	468	13,010	70	15,840–15,240	−3.1
GrN-31210	Carbonate	505	16,840	120	19,790–19,450	+1.1

AMS, Accelerator mass spectrometry; *BP*, Before Present;*, not calibrated.

curve and reflected as a slight increase in the *Betula* curve.

Similar oscillations in pollen diagrams of Late Glacial lake deposits in the Alpine region have been published by Bortenschlager (1984).

3.3.3 Radiocarbon stratigraphy

Radiocarbon dating of calcareous gyttja is problematic because it easily overestimates ages due to reservoir effects (Mook and Streurman, 1983), which are difficult to quantify. We could obtain reliable dates for a few (bulk) peat samples of Gasserplatz core 2, in addition to two 'anchor points' (the onset of the Younger Dryas and the LST) to obtain a reliable chronology.

Various samples of Gasserplatz core 1, consisting of peaty gyttja, calcareous gyttja and molluscs, were selected for radiocarbon dating. The results are shown in Table 3.3.1 and Fig. 3.3.11. The peat sequence (red in Fig. 3.3.11) shows a linear relation with time (calibrated ^{14}C dates).

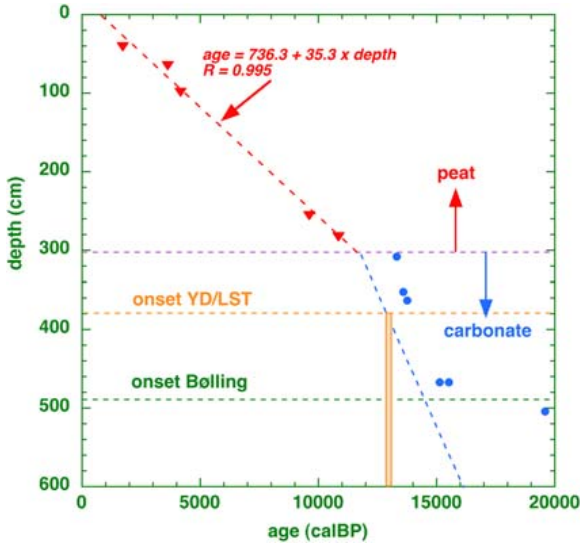

FIGURE 3.3.11 Calibrated ^{14}C dates as a function of depth for Gasserplatz. *After van Mourik, J.M., Slotboom, R.T., van der Plicht, J., Streurman, H.J., Kuijper, W.J., Hoek, W.Z., de Graaff, L.W.S., 2013. Geochronology of Betula extensions in pollen diagrams of Alpine Late-glacial lake deposits: a case study of the Late-glacial deposits of the Gasserplatz soil archives (Vorarlberg, Austria). Quaternary International 306, 3–13.*

The starting time of the peat is at a depth of 306 cm, corresponding to a calibrated age of 11,550 calBP. This point is also the end point of the carbonate set of dates obtained from the gyttja.

The timeline for the carbonates can be constructed from this point and the other horizons as 'anchor points': the onset of the Younger Dryas (YD) and Laacher See Tephra (LST) at 380 and 383 cm, respectively, and the onset of Bølling (490 cm depth, 14,500 calBP).

LST is identified in the sequence at a depth of 383 cm. From the laminated Meerfelder Maar sequence in the Eifel, it appears that LST was deposited some 190 years before the onset of the Younger Dryas (Brauer et al., 1999).

All carbonates (blue in Fig. 3.3.11) are subjected to reservoir effects, as can be seen from their deviation from the deposition line. Even a peat sample at 386 cm depth shows a (small) reservoir effect. It shows a very negative $\delta^{13}C$ value of $-32.4‰$ caused by submerged plants.

3.3.4 Stable isotope stratigraphy

For both Gasserplatz series, the stable isotope ratios ($\delta^{13}C$ and $\delta^{18}O$) of the carbonate fractions are shown in Fig. 3.3.12A and B as a function of depth. They overlap, and the Younger Dryas cold reversal is clearly visible. These data lead to the following observations.

In general terms, the organic production (plant growth) determines the $\delta^{13}C$ of the carbonate in the system, and thus the size of the reservoir effect for ^{14}C dates. Plants are in isotopic equilibrium with the carbonates. Further biological production leads to higher CO_2 concentration and consequently a more negative $\delta^{13}C$ for submerged plants and carbonates. For example, for the sample at a depth of 422 cm, the $\delta^{13}C$ for the organic material was $-38‰$, and for the carbonate $-6‰$.

There is a clear relationship between $\delta^{13}C$ and $\delta^{18}O$ (Fig. 3.3.12A and B). Lower temperatures (lower $\delta^{18}O$ values) correlate with more negative

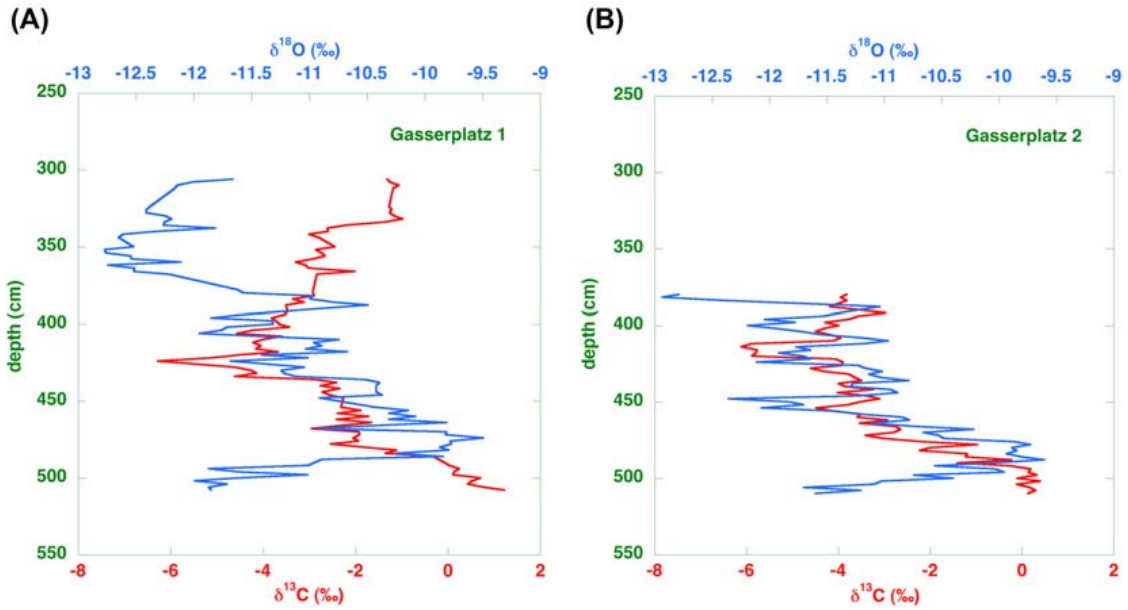

FIGURE 3.3.12 (A). Isotope stratigraphy of Gasserplatz-1. (B). Isotope stratigraphy of Gasserplatz-2. *After van Mourik, J.M., Slotboom, R.T., van der Plicht, J., Streurman, H.J., Kuijper, W.J., Hoek, W.Z., de Graaff, L.W.S., 2013. Geochronology of Betula extensions in pollen diagrams of Alpine Late-glacial lake deposits: a case study of the Late-glacial deposits of the Gasserplatz soil archives (Vorarlberg, Austria). Quaternary International 306, 3–13.*

$\delta^{13}C$ values, and are related to higher water levels caused by higher rain- and groundwater input. In contrast, the warmer periods mean less water input, a lower water level and evaporation, yielding more positive $\delta^{13}C$ and $\delta^{18}O$ values. During the cold period before 16,000 there is no biological activity in the system, which is consistent with the observation of higher reservoir effects (Fig. 3.3.11).

The oxygen isotope stratigraphy shown in Fig. 3.3.12B is consistent with the one shown in Fig. 3.3.12A. The climate proxy signals show a similar trend in both cores. Together with the ^{14}C-derived deposition plot, the stratigraphic framework of the stable isotopes is used to support the chronology of the Late Glacial section of the Gasserplatz records. This approach has been used successfully at other locations (Von Grafenstein et al., 1999; Schwander et al., 2000; Hoek and Bohncke, 2001; Lotter et al., 1992, 2012).

We conclude that the pollen records of the Gasserplatz show a clear registration of Late Glacial oscillations, probably caused by climatic oscillations. Radiocarbon dates overestimate the age of calcareous lake sediments and cannot be used to establish the geochronology of these climatic oscillations. This is caused by reservoir effects, for which the stable isotopes $\delta^{13}C$ and $\delta^{18}O$ of the carbonate fraction provide information.

The oxygen isotope chronology of the Gasserplatz records correlates with the *Betula* oscillations and with the oxygen isotope stratigraphy of the Greenland ice cores.

3.4 Dating of vegetation horizons

Similar to soils, for vegetation horizons, the humic acid fraction is the best datable fraction for radiocarbon dating. As an example we consider the Schildmeer (in the province of Groningen, the Netherlands). A series of dates is shown in Tables 3.4.1 and 3.4.2 for two locations named S230 and S123.

Only two separate layers (named I and II) are observed in clay above a peat layer, which is very common in the region (Schoute, 1985).

The data are a summary based on the observations made by Schoute (1985). In general, the C content is low for these samples. Therefore

TABLE 3.4.1 Dating fractions from vegetation horizons from Schildmeer (S230).

Type	Lab code	Fraction	Sample (g)	Ash (g)	Carbon (g)	Cpr (%)	Cv (%)	^{14}C age (BP)	Sigma	$\delta^{13}C$ (‰)
Clay	GrN-9520	Humic acid	4.02	0.25	1.90	47	50	2260	50	−27.35
Clay	GrN-9519	Humin	185.6	172.4	3.11	2	24	2395	35	−27.46
Top vh I	GrN-9516	Humic acid	100.0	72.0	14.0	14	50	1975	20	−27.29
Top vh I	GrN-9515	Humin	152.0	138.0	6.79	45	48	2150	30	−26.70
Bottom vh I	GrN-9514	Humic acid	43.4	31.3	5.71	13	47	2350	30	−25.68
Bottom vh I	GrN-9513	Humin	198.0	187.9	2.55	1	25	2845	50	−26.71
Clay	GrN-9518	Humic acid	7.7	3.10	2.26	29	49	2815	55	−24.52
Clay	GrN-9517	Humin	160.0	143.2	4.81	3	28	2800	30	−27.41

Cpr, relative amount of carbon after pretreatment; *Cv*, (amount of C)/(amount of sample minus amount of ash) * 100%.

TABLE 3.4.2 Dating fractions from vegetation horizons from Schildmeer (S123).

Type	Lab code	Fraction	Sample (g)	Ash (g)	Carbon (g)	Cpr (%)	Cv (%)	^{14}C age (BP)	Sigma	δ^{13}C (‰)
Clay	GrN-9502	Humic acid	1,4	0.2	0.6	42	49	1280	60	−26.90
Clay	GrN-9501	Humin	242.0	22.9	2.9	1	22	1355	45	−26.69
vh II	GrN-8981	Humic acid	92.4	80.8	4.57	5	39	1665	25	−29.18
vh II	GrN-8980	Humin	282.7	270.0	2.12	1	17	2050	60	−28.18
Top vh I	GrN-8979	Humic acid	40.3	31.3	4.71	12	52	2015	25	−26.89
Top vh I	GrN-8978	Humin	162.0	155.2	2.04	1	30	2200	60	−27.43
Bottom vh I	GrN-8977	Humic acid	43.3	28.8	4.71	11	32	2210	25	−27.17
Bottom vh I	GrN-8976	Humin	144.0	133.6	4.16	3	40	2410	80	−27.58
Clay	GrN-9500	Humic acid	3.8	0.05	1.9	51	51	2935	55	−24.58
Clay	GrN-8982	Humin	219.0	203.0	3.0	1	19	2730	60	−25.69

Cpr, relative amount of carbon after pretreatment; *Cv*, (amount of C)/(amount of sample minus amount of ash) * 100%.

the risk for contamination is large. The humin fraction contains the allochthonous carbon, mostly from marine clay sediment consisting of fine particles of reworked peat.

As a function of depth we observe the following for S123:

GrN-9502/9501 is taken from clay, GrN-8981/8980 the upper vegetation horizon (VH2); for the lower vegetation horizon (VH1) GrN-8979/8978 is from the top and GrN-8977/8976 is from the bottom. The next clay layer yields GrN-9500/9501. For the region, the underlying peat is dated to ca. 2600 BP (GrN-8961/8960) (not shown in the table).

The vegetation horizons above the peat show a reasonable stratigraphy for the humic acid fraction; the humin dates appear to be unreliable. The lowest clay fraction also yields an impossible date.

For S230, also as a function of depth:

GrN-9520/9519 is taken from clay; GrN-9516/9515 and 9514/9513 represent the top and bottom of VH1. Also here, the underlying peat is dated to ca. 2600 BP (GrN-8961/8960) (not shown in the table).

3.5 Dating of bog peat

Raised bogs from the eastern Netherlands (Meerstalblok, Engbertsdijkveen and others) have been studied extensively. This concerns botanical analysis as well as ^{14}C dating and interpretation of δ^{13}C values (Blaauw, 2003 and references therein).

Fig. 3.5.1 shows the δ^{13}C values of aboveground remains from several bog plant species. It illustrates the influence of wet/dry conditions quite well. *Sphagnum cuspidatum* represents wet conditions, with high δ^{13}C values. Plants representing dry conditions (like *Calluna vulgaris*) show low δ^{13}C values; wetter conditions correspond to higher δ^{13}C values. For more details we refer to Blaauw et al. (2004).

The datable fraction for peat bogs is the humin fraction; the humic acids generally show rejuvenation. Organic matter from peat bogs is chemically pretreated by the standard AAA method (Mook and Streurman, 1983). Note that soils are the exception for this procedure. Contamination problems do play a role for

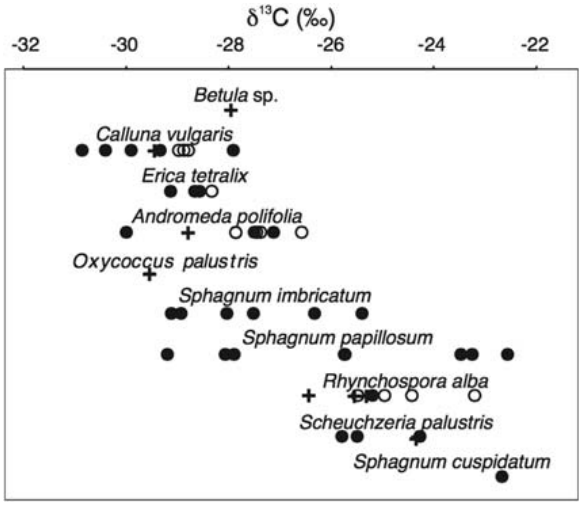

FIGURE 3.5.1 The $\delta^{13}C$ values of raised bog plant species. *From Blaauw, M., 2003. An Investigation of Holocene Sun-Climate Relationships Using Numerical ^{14}C Wiggle Match Dating of Peat Deposits. PhD thesis, University of Amsterdam.*

dating of peat, in particular the Pleistocene age (e.g., van der Plicht, 2012).

Bulk peat sample dating was the only possibility during the conventional era. The introduction of AMS enabled ^{14}C dating of small samples, which for peat can be translated into selected macrofossils or seeds (Blaauw, 2003 and references therein). This solved dating problems caused by mobile organic fractions, and the consensus that *Sphagnum* plant fragments should be used in ^{14}C dating of peat (e.g., Nilsson et al., 2001).

Fig. 3.5.1 shows results for species-specific plants. Bulk dates (not species specific) of peat bogs show different $\delta^{13}C$ values of hummocks and hollows determined by dry/wet conditions. An example for Engbertdijksveen is shown in Fig. 3.5.2, which shows such $\delta^{13}C$ values between 1000 and 3500 BP. The data and references can be found in Blaauw (2003).

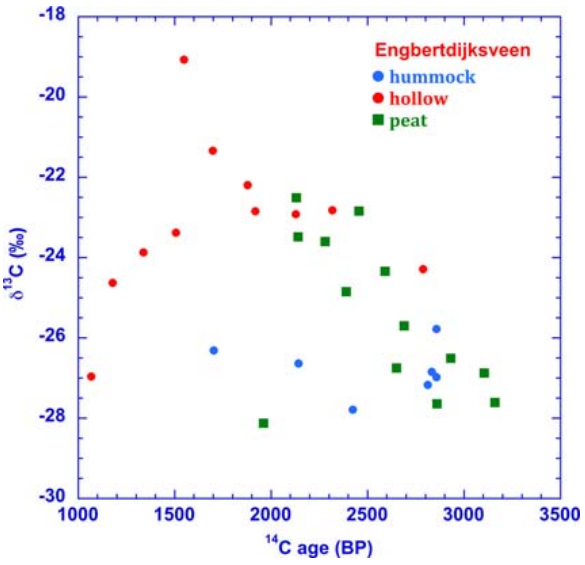

FIGURE 3.5.2 The $\delta^{13}C$ values of hummocks and hollows for the peat bog Engbertdijksveen.

3.6 Conclusions

Radiocarbon dating of organic samples is usually very successful, provided the correct datable fraction is prepared and contamination is removed. Soil organic carbon is complicated matter for dating.

In general, the humic acid fraction is considered the correct datable fraction for soil organic carbon but also the humin fraction provides information about the development of soil and landscape.

The stable isotope ^{13}C can be used as a tracer for soil formation processes. The $\delta^{13}C$ value yields information on aquatic plants and wet/dry conditions, depending on type of organic deposit. Application of both carbon isotopes in soil science is illustrated by selected case studies showing the interpretation of fractionated radiocarbon dating and the added value of the $\delta^{13}C$ data.

References

Aerts, A.T., van der Plicht, J., Meijer, H.A.J., 2001. Automatic AMS sample combustion and CO_2 collection. Radiocarbon 43, 293–298.

Bayliss, A., McCormac, A.G., van der Plicht, J., 2004. An illustrated guide to measuring radiocarbon from archaeological samples. Physics Education 39, 1–8.

Blaauw, M., 2003. An Investigation of Holocene Sun-Climate Relationships Using Numerical ^{14}C Wiggle Match Dating of Peat Deposits. PhD thesis. University of Amsterdam.

Blaauw, M., van der Plicht, J., van Geel, B., 2004. Radiocarbon dating of bulk peat samples from raised bogs: non-existence of a previously reported reservoir effect? Quaternary Science Reviews 23, 1537–1542.

Bortenschlager, S., 1984. Die Vegetationsentwicklung im Spätglazial. Das Moor beim Lanser See III, ein Typprofil für die Ostalpen. Dissertationes Botanicae 72, 71–79.

Brauer, A., Endres, C., Gunter, C., Litt, T., Stebich, M., Negendank, J.F.W., 1999. High resolution sediment and vegetation responses to Younger Dryas climate change in varved lake sediments from Meerfelder Maar, Germany. Quaternary Science Reviews 18, 321–329.

Brewer, R., 1976. Fabric and Mineral Analysis of Soils. Robert E. Krieger Publishing Company, Huntingon, New York, 482pp.

Bronk Ramsey, C., Staff, R.A., Bryant, C.L., Brock, F., Kitagawa, H., van der Plicht, J., Schlolaut, G., Marshall, M.H., Brauer, A., Lamb, H.F., Payne, R.L., Tarasov, P.E., Haraguchi, T., Gotanda, K., Yonenobu, H., Yokoyama, Y., Tada, R., Nakagawa, T., 2012. A complete terrestrial radiocarbon record for 11.2 to 52.8 kyr BP. Science 338, 370–374.

Bucha, V., 1970. Influence of the Earth's magnetic field on Radiocarbon dating. In: Olsson, I.U. (Ed.), Radiocarbon Variations and Absolute Chronology. Proceedings of The 12th Nobel Symposium. Wiley, pp. 501–511.

Castel, I.I.Y., Koster, E.A., Slotboom, R.T., 1989. Morphogenetic aspects and age of late Holocene drift sand in northwest Europe. Zeitschrift für Geomorphologie, Neu Folge 33, 1–26.

Cook, G.T., van der Plicht, J., 2013. Radiocarbon dating. In: Encyclopedia of Quaternary Science, second ed. Elsevier, Amsterdam, pp. 305–315.

de Graaff, L.W.S., Kuijper, W.J., Slotboom, R.T., 1989. Schlussvereisung und spätglaziale Entwicklung des Moorgebietes Gasserplatz (Feldkirch-Göfis, Vorarlberg). In: Jahrbuch der Geologischen Bundesanstalt, Band, vol. 132, pp. 397–413.

de Vries, H., 1958. Variation in concentration of radiocarbon with time and location on earth. Proceedings KNAW B61, 1–9.

Dijkmans, J.W.A., van Mourik, J.M., Wintle, A.G., 1992. Thermoluminescence dating of aeolian sands from polycyclic soil profiles in the Southern Netherlands. Quarternary Science Reviews 11, 85–92.

Ellis, S., Matthews, J.A., 1984. Pedogenetic implications of a 14C-dated paleopopodzolic soil at Haugabreen, Southern Norway. Arctic and Alpine Research 16, 77–91.

Fry, B., 2008. Stable Isotope Ecology. Springer.

Godwin, H., 1962. Halflife of radiocarbon. Nature 195, 984.

Goh, K.M., Molloy, B.P.J., 1978. Radiocarbon dating of paleosols using soil organic matter components. Journal of Soil Science 29, 567–573.

Graven, H.D., 2015. Impact of fossil fuel emissions on atmospheric radiocarbon and various applications of radiocarbon over this century. Proceedings of the National Academy of Sciences United States of America 112, 9542–9545.

Groenman-van Waateringe, W., 1988. Palynologisch onderzoek van het urnenveld te Weert. KNAG Netherlands Geographical Studies 74, 139–156.

Hoek, W.Z., Bohncke, S.J.P., 2001. Oxygen-isotope wiggle-matching as a tool for correlation of ice-core and terrestrial records over termination I. Quaternary Science Reviews 20, 1251–1264.

Hua, Q., Barbetti, M., Rakowski, A.Z., 2013. Atmospheric radiocarbon for the period 1950–2010. Radicoarbon 55, 2059–2072.

Johnsen, S.J., Dahl-Jensen, D., Gundestrup, N., Steffensen, J.P., Clausen, H.B., Miller, H., Masson-Delmotte, V., Sveinbjornsdottir, A., White, J., 2001. Oxygen isotope and palaeotemperature records from six Greenland ice core stations: camp century, GRIP, GISP2, Renland and NorthGRIP. Journal of Quaternary Science 16, 299e307.

Jull, A.J.T., 2013. AMS method. radiocarbon dating. In: Elias, S.A. (Ed.), Encyclopedia of Quaternary Science, second ed. Elsevier, Amsterdam, pp. 2911–2918.

Lanting, J.N., van der Plicht, J., 1994. 14C-AMS: pros and cons for archaeology. Palaeohistoria 35/36, 1–12.

Levin, L., Hesshaimer, V., 2000. Radiocarbon, a unique tracer of global carbon cycle dynamics. Radiocarbon 42, 69–80.

Libby, W.F., 1952. Radiocarbon Dating. University of Chicago Press.

Lotter, A.F., Eicher, U., Siegentahler, U., Birks, H.J., 1992. Late-glacial climatic oscillations as recorded in Swiss lake sediments. Journal of Quaternary Science 7, 187–204.

Lotter, A.F., Heiri, O., Brooks, S., van Leeuwen, J.N., Eicher, U., Ammann, B., 2012. Rapid summer temperature changes during termination 1a: high resolution multi-proxy climate reconstructions from Gerzensee (Switzerland). Quaternary Science Reviews 36, 103–113.

Meadows, J., 2005. The younger Dryas episode and the radiocarbon chronologies of the lake Huleh and Ghab valley pollen diagrams, Israel and Syria. The Holocene 15, 631–636.

Michener, R., Lajtha, K.R., 2007. Stable Isotopes in Ecology and Environmental Science. Blackwell, Oxford.

Mook, W.G., 2006. Introduction to Isotope Hydrology: Stable and Radioactive Isotopes of Hydrogen, Oxygen and Carbon. Taylor and Francis, London.

Mook, W.G., Streurman, H.J., 1983. Physical and chemical aspects of radiocarbon dating. PACT Publications 8, 31–55.

Mook, W.G., Waterbolk, H.T., 1985. Handbooks for Archaeologists No.3: Radiocarbon Dating. European Science Foundation. ISBN 2-903148-44-9.

Mook, W.G., van de Plassche, O., 1986. Radiocarbon dating. In: van de Plassche, O. (Ed.), Sea Level Research: A Manual for the Collection and Evaluation of Data. Geo Books. Norwich525-560.

Mook, W.G., van der Plicht, J., 1999. Reporting 14C activities and concentrations. Radiocarbon 41, 227–239.

Moore, P.D., Webb, J.A., Collinson, M.E., 1991. Pollen Analyses. Blackwell, Oxford, p. 216.

Nilsson, M., Klarqvist, M., Bohlin, E., Possnert, G., 2001. Variation in 14C age of macrofossils and different fractions of minute peat samples dated by AMS. The Holocene 11, 579–586.

Olsson, I.U., 1983. Dating non-terrestrial materials. PACT Publications 8, 277–294.

Olsson, I.U., 1989. The 14C method, its possibilities and some pitfalls. PACT Publications 24, 161–177.

Reimer, P.J., Bard, E., Bayliss, A., Beck, J.W., Blackwell, P.G., Bronk Ramsey, C., Buck, C.E., Edwards, R.L., Friedrich, M., Grootes, P.M., Guilderson, T.P., Haflidason, H., Hajdas, I., Hatté, C., Heaton, T.J., Hoffmann, D.L., Hogg, A.G., Hughen, K.A., Kaiser, K.F., Kromer, B., Manning, S.W., Niu, M., Reimer, R.W., Richards, D.A., Scott, E.M., Southon, J.R., Staff, R.A., Turney, C.S.M., van der Plicht, J., 2013. IntCal13 and Marine13 Radiocarbon age calibration curves 0-50,000 years cal BP. Radiocarbon 55, 1869–1887.

Reimer, P.J., Austin, W.E.N., Bard, E., Bayliss, A., Blackwell, P.G., Bronk Ramsey, C., Butzin, M., Cheng, H., Edwards, L., Friedrich, M., Grootes, P.M., Guilderson, T.P., Hajdas, I., Heaton, T.J., Hogg, A.G., Hughen, K.A., Kromer, B., Manning, S.W., Muscheler, R., Palmer, J.G., Pearson, C., van der Plicht, J., Reimer, R.W., Richards, D., Scott, E.M., Southon, J.R., Turney, C.S.M., Wacker, L., Adophi, F., Büntgen, U., Capano, M., Fahrni, S., Fogtmann-Schulz, A., Friedrich, R., Kudsk, S., Miyake, F., Olsen, J., Reinig, F., Sakamoto, M., Sookdeo, A., Talamo, S., 2020. The IntCal20 Northern Hemisphere radiocarbon calibration curve (0-55 kcal BP). Radiocarbon (in press).

Riede, F., 2008. The Laacher See-eruption (12,920 BP) and material culture change at the end of the Allerød in northern Europe. Journal of Archaeological Science 35, 591–599.

Schoute, J.F.T., 1985. Vegetation Horizons and Related Phenomena. PhD thesis, VU, Amsterdam.

Schwander, J., Eicher, U., Ammann, B., 2000. Oxygen isotopes of lake marl at Gerzensee and Leysin (Switzerland), covering the Younger Dryas and two minor oscillations, and their correlation to the GRIP ice core. Palaeogeography, Palaeoclimatology, Palaeoecology 159, 203e214.

Scott, E.M., Cook, G.T., Naysmith, P., 2010. The Fifth International Radiocarbon Intercomparison (VIRI): an assessment of laboratory performance in stage 3. Radiocarbon 52, 859–865.

Simons, A.L., 1985. Geomorphologische und glazialgeologischeUntersuchungen in Vorarlberg, Österreich. In: Schriften des VorarlbergerLandesmusums, Reihe A, Band, vol. 1, p. 57.

Stevenson, F.J., 1985. Geochemistry of soil humic substances. In: Humic Substances in Soil Sediment and Water. Wiley, New York, pp. 13–53.

Stuiver, M., 1965. Carbon-14 content of 18th- and 19th-century wood: variations correlated with sunspot activity. Science 149, 533–534.

Stuiver, M., Quay, P., 1981. Atmospheric 14C changes resulting from fossil fuel CO_2 release and cosmic ray flux variability. Earth and Planetary Science Letters 53, 249–362.

Suess, H.E., 1980. The radiocarbon record in tree rings of the last 8000 years. Radiocarbon 22, 200–209.

Taylor, R.E., Long, A., Kra, R.S., 1992. Radiocarbon after Four Decades: An Interdisciplinary Perspective. Springer Verlag, New York.

Trumbore, S.E., Vogel, J.S., Southon, J.R., 1989. AMS measurements of fractionated soil organic matter: an approach to deciphering the soil carbon cycle. Radiocarbon 31, 644–654.

Tuniz, C., Kutschera, W., Fink, D., Herzog, G.F., Bird, J.R., 1998. Accelerator Mass Spectrometry: Ultrasensitive Analysis for Global Science. CRC press. ISBN 9780849345388.

van der Plicht, J., 2012. Borderline radiocarbon. Netherlands Journal of Geosciences 91, 257–261.

van der Plicht, J., 2013. Variations in atmospheric 14C. In: Elsevier Encyclopedia of Quaternary Science, 2nd, revised edition, pp. 329–335.

van der Plicht, J., Bruins, H.J., 2001. Radiocarbon dating in Near-Eastern Mediterranean contexts: confusion and quality control. Radiocarbon 43, 1155–1166.

van der Plicht, J., Hogg, A., 2006. A note on reporting radiocarbon. Quaternary Geochronology 1, 237–240.

van der Plicht, J., Wijma, S., Aerts, A.T., Pertuisot, M.H., Meijer, H.A.J., 2000. The Groningen AMS facility: status report. Nuclear Instruments and Methods B 172, 58–65.

van der Plicht, J., Streurman, H.J., Bottema, S., Mook-Kamps, E., 2001/2002. Wildervank: an investigation using natural isotopes. Palaeohistoria 43/44, 35–42.

van Mourik, J.M., 1988. De ontwikkeling van een stuifzandgebied. KNAG Netherlands Geographical Studies 74, 5–42.

van Mourik, J.M., Wartenbergh, P.E., Mook, W.G., Streurman, H.J., 1995. Radiocarbon dating of palaeosols in aeolian sands. Mededelingen Rijks Geologische Dienst 52, 425–440.

van Mourik, J.M., Nierop, K.G.J., Vandenberghe, D.A.G., 2010. Radiocarbon and optically stimulated luminescence dating based chronology of a polycyclic driftsand sequence at Weerterbergen (SE Netherlands). Catena 80, 170–181.

van Mourik, J.M., Seijmonsbergen, A.C., Jansen, B., 2012a. Geochronology of Soils and Landforms in Cultural Landscapes on Aeolian Sandy Substrates, Based on Radiocarbon and Optically Stimulated Luminescence Dating (Weert, SE-Netherlands). Intech Radiometric dating, pp. 75–114.

van Mourik, J.M., Seijmonsbergen, A.C., Slotboom, R.T., Wallinga, J., 2012b. The impact of human land use on soils and landforms in cultural landscapes on aeolian sandy substrates (Maashorst, SE Netherlands). Quaternary International 265, 74–89.

van Mourik, J.M., Slotboom, R.T., van der Plicht, J., Streurman, H.J., Kuijper, W.J., Hoek, W.Z., de Graaff, L.W.S., 2013. Geochronology of Betula extensions in pollen diagrams of Alpine Late-glacial lake deposits: a case study of the Late-glacial deposits of the Gasserplatz soil archives (Vorarlberg, Austria). Quaternary International 306, 3–13.

van Strydonck, M., Nelson, D.E., Combré, P., Bronk Ramsey, C., Scott, E.M., van der Plicht, J., Hedges, R.E.M., 1999. What's in a 14C date. In: Proceedings Third Conference on 14C and Archaeology, pp. 433–440. Lyon (France).

Vera, H., 2011. 'Dat men het goed van de ongeboornen niet mag verkoopen'; Gemene gronden in de Meierij van Den Bosch tussen hertog en hertgang 1000 – 2000. Uitgeverij BOXpress, Oisterwijk, Netherlands (with english summary).

von Grafenstein, U., Erlenkeuser, H., Brauer, A., Jouzel, J., Johnsen, S.J., 1999. A mid-European decadal isotope-climate record from 15,500 to 5000 years BP. Science 284, 1654–1657.

Wagner, T.V., Mouter, A.K., Parsons, J.R., Sevink, J., van der Plicht, J., Jansen, B., 2018. Molecular characterization of charcoal to identify adsorbed SOM and assess the effectiveness of common SOM-removing pre-treatments prior to radiocarbon dating. Quaternary Geochronology 45, 74–84.

Wallinga, J., van Mourik, J.M., Schilder, M.L.M., 2013. Identifying and dating buried micropodzols in Subatlantic polycyclic drift sands. Quaternary International 306, 60–70.